IEEE Access
Multidisciplinary | Rapid Review | Open Access Journal

Received December 3, 2020, accepted December 19, 2020, date of publication December 28, 2020, date of current version January 7, 2021.

*Digital Object Identifier 10.1109/ACCESS.2020.3047698*

# Dynamic Pose Tracking Performance Evaluation of HTC Vive Virtual Reality System

**MOHAMED SADIQ IKBAL, VISHAL RAMADOSS, (Member, IEEE), AND MATTEO ZOPPI**
PMAR Robotics Group, Department of Mechanical, Energy, Management, and Transportation Engineering, University of Genoa, 16145 Genoa (GE), Italy
Corresponding author: Mohamed Sadiq Ikbal (mohamedsadiq.ikbal@edu.unige.it)

**ABSTRACT** Virtual reality tracking devices are rapidly becoming the go-to system for cost-effective motion tracking solutions across different communities such as robotics, biomechanics, sports, rehabilitation, motion simulators, etc. This article focuses on the spatial tracking performance of HTC Vive's lighthouse tracking system (VLTS) devices (tracker, controller, and head mount display). A comprehensive literature survey on the performance analysis of VLTS on the various aspects is presented along with its shortcomings in terms of spatial tracking evaluation. The two key limitations have been identified: in static cases, there is a lack of standard procedures and criteria, and in dynamic cases, the entire study of spatial tracking. We address the first by assessing VLTS using the optical tracking system standard specified by ASTM International, and the latter by revising the standards to determine the upper-velocity limit for reliable tracking. The findings are substantiated with the trajectories of human wrist motion. Each evaluation's results are systematically analyzed with statistical hypothesis tests and criteria fulfillment. Comau NS16, an industrial serial robot, was used as the ground truth motion generator due to its repeatability and 6 degrees of workspace freedom. One of the major reasons for not having more generalized spatial tracking studies is that the tracking performance heavily depends on the configurations of the setup, work volume, environment, etc. Thus, the guidelines for configuring VLTS and the approach adapted from ASTM standards for evaluating VLTS for custom applications using our reported findings for both static and dynamic cases are included in the appendix.

**INDEX TERMS** Lighthouse tracking, motion tracking, performance evaluation and bench-marking, virtual reality and interfaces.

## NOMENCLATURE

| | |
|---|---|
| VLTS | HTC Vive's lighthouse tracking system. |
| BS | Base station of HTC Vive. |
| HMD | Head mount display of HTC Vive. |
| T | Tracker device of HTC Vive. |
| C | Controller device of HTC Vive. |
| DOF | Degree of freedom. |
| MOCAP | Motion capture system. |
| ASTM | ASTM International. |
| $d_{BS}$ | Distance between base stations. |
| $e_{AD}$ | Average distance error. |
| $\sigma$ | Standard deviation of error. |
| RMSE | Root mean square error. |
| C16 | Comau NS16 1.65 foundry hand industrial serial robot. |
| RMSD | Root mean square deviation. |
| E(95) | Expected error at 95 percentile. |
| E(97) | Expected error at 97 percentile. |
| E(99.7) | Expected error at 99.7 percentile. |
| AET | Average error test. |
| MPET | Maximum permissible error test. |
| $\bar{d}$ | Average measurement deviation from mean. |
| $d_{max}$, $d_{min}$ | Maximum and minimum measurement deviation from mean. |
| $\bar{e}$ | Average measurement error. |
| $e_{max}$, $e_{min}$ | Maximum and minimum measurement error. |
| $\delta_{avg}$ | Expected average error/deviation from mean. |
| $\delta_{max}$ | Expected maximum error/deviation from mean. |
| $H_o$ | Null hypothesis of the hypothesis tests. |
| $H_a$ | Alternative hypothesis of the hypothesis tests. |
| N | Sample size of measured data. |
| $s^2$ | Variance of measured error. |

The associate editor coordinating the review of this manuscript and approving it for publication was Tai-Hoon Kim.

| | |
|---|---|
| ${}_{Left}H_{Right}$ | Homogenous transformation matrix of right object with respect to the left in VLTS' coordinate frame. |
| ${}_{Left}\hat{H}_{Right}$ | Homogenous transformation matrix of right object with respect to the left in C16' coordinate frame. |
| P | Position/linear degree of freedom. |
| O | Orientation/angular degree of freedom. |
| CDF | Cummulative distribution function. |
| %Loss | Percentage loss of tracking. |

## I. INTRODUCTION

Virtual reality (VR) motion tracking devices have been serving as a low-cost motion tracking solutions for both the VR and non-VR application like robotics, scientific research, motion capture, motion simulators, mixed reality video production, medical science, rehabilitation, interactive art, etc., since its market debut in 2016. Each VR consumer product company makes its custom motion tracking systems, such as the VLTS [1], Oculus sensor [2], camera-based, insight tracking [3], etc. There are various tracking technologies that have different physical operating principles [4]. The technique most adapted for consumer VR products are outside-in tracking [5] and inside-out tracking [6]. Although VR's major issue of portability is solved by inside-out, at the time of writing this article outside-in acts as a gold standard for VR motion tracking due to its better tracking performance [7]. Thus, the focus of this article is on the first and most widely used commercial outside-in tracking system, the HTC VIVE's lighthouse tracking system.

HTC Vive comes with two base stations, one head mount display, two controllers, and trackers. VLTS enables tracking of these devices in six DOF with reference to a common frame calibrated at initial setup process. The working principles and other setup considerations are explained in section II-A.

A detailed performance metrics of VLTS are not provided by the developers [15], as it is a VR utility device. Upon gaining popularity as an affordable motion tracking alternative, various studies investigated its performance either in general or for a specific application. Table 1 provides a summary of studies investigating the spatial tracking performance of VLTS. In [8], the possibility of using tracker as a ground truth tracking system was examined and an algorithm was presented using only the light data to improve dynamic performance sacrificing precision in static cases. The precision evaluation of the controller against the Vicon MOCAP for clinical research was conducted by [9]. The static performance of HMD was evaluated by [10] with grid lines drawn on the floor for three different tracking volumes for scientific research. Another static evaluation similar to [10] with more accurate ground truth was conducted by [11]. The precision analysis for rehabilitation and medical tracking purposes was conducted by [12] and [13]. Usage of the controller for automated testing of an industrial robot was assessed by [14].

There are few references assessing Vive system with criteria other than spatial tracking. Time performance assessment (latency and jitter) for neuroscience and biofeedback studies under strong time constraints ($< 10\ ms$) was made in [16], proving that events less than 22 ms cannot be registered. Performance bound assessment of lighthouse positioning system against the ultra-wide band for micro unmanned aerial vehicles was conducted in [17], showing that the earlier is a viable option. The ability to extend the tracking space of lighthouse tracking system in general was examined in [18]. The quality of experience of the Vive and Oculus Rift systems was compared in [19], concluding that the Vive is marginally better. Numerous studies using Vive as one of the setup devices is not included in this survey, as it is beyond the scope of this article.

This article aims to address the two potential shortcomings of the current literature presented in Table 1: First, the results of the performance evaluation differ based on the setup. For instance, [8] reports precision in millimeter whereas [13] and [14] report sub-millimeter precision. The similar ambiguity can be observed in static analysis as well, all articles report sub-millimeter accuracy except for [11] and [12]. The results of [11] are higher because the configuration of tracking space is larger than the recommended 5 m, as the author was testing for extreme cases. The poor static performance of [12] could be due to the interference of infrared from their ground truth system Vicon MOCAP, as we experienced the same issue of inaccuracy during our initial testing of Vive with Optitrack MOCAP as ground truth system. These variation in reports is due to a lack of standard procedures to compare performance across various applications. VLTS being a hybrid system with multiple sensor data fused to make the VR experience smooth in terms of human-motion perception has no predefined/available standard. In this article, we attempt to standardize the VLTS' motion tracking evaluation by considering the ASTM International standard [20] for bench-marking optical tracking devices with markers. The nominal reference for precision evaluation, static, and dynamic analysis were chosen as [21], [22], and [23] respectively. These standards were selected because the key percentage of VLTS' data is from lighthouse tracking with photo-diode sensors [24].

Second, as it is evident from Table 1, most of the literature conduct the precision evaluation and static analysis for their different intended applications but there is a lack of performance evaluation under dynamic motion states. Although [8] compared their algorithm with off-the-self Vive's algorithm under motions with a velocity ranging between 10 to 60 mm/s, it does not provide the VLTS's dynamic pose tracking performance. Since most applications require spatial tracking under the broad range of motions with different velocity intensities, it is essential to have clearer and comprehensive performance statistics of VLTS under various dynamic conditions. In this article, we conduct an in-depth dynamic pose tracking analysis which includes the standardized evaluation as per the protocols in [23], determination of upper bound velocity of reliable tracking, examining

**TABLE 1. Summary of existing Vive evaluation studies.**

| Ref. | Device | Space calibration | Precision evaluation | Static analysis | Dynamic analysis | Ground truth system | Intended application |
|---|---|---|---|---|---|---|---|
| [8] | T | $d_{BS}$: 1) 93 mm, 2) 6271 mm | 1) $\sigma$ = 5 mm, 2) $\sigma$ = 28 mm | $\sigma_{lin} < 0.5$ mm, $\sigma_{ang} < 0.006°$ | Velocity range = 10 - 60 mm/s | Astrobee robot | Robotics |
| [9] | C | 1) Room scale, 2)Standing | – | $e_{AD}$: 1) 0.74±0.42 mm, 0.46±0.46°; 2) 0.63±0.27 mm, 0.66±0.40° | – | UR5 robot with Vicon MOCAP | Clinical research |
| [10] | HMD | $d_{BS}$: 1) 7.45 m, 2) 5 m, 3) 5.66 m | – | RMSE: 1) < 0.08 mm, < 0.0111°, 2) < 0.064 mm, < 0.0113°, 3) < 0.066 mm, < 0.0053° | – | Grid lines on floor with String and Chalk (positioning error, $\sigma$ = 17 mm) | VR for scientific research |
| [11] | T, C, HMD | $d_{BS}$ : 1) 7.6 m, 2) 6.3 m | – | T: 1) $\sigma$ < 2.81 mm 2) $\sigma$ < 2.85 mm C Left: RMSE 1) 14.42 mm, 2) 5.15 mm; C Right: RMSE 1) 9.15 mm, 2) 8.81 mm, HMD: RMSE = 1) 11.48 mm 2) 7.93 mm | – | Phase Space MOCAP | Similar to [10] with accurate ground truth |
| [12] | T | Tracking volume: 2.5 × 2.5 m | – | RMSE: 6.8±3.2 mm, 1.64±0.18° | – | Vicon MOCAP with 1) SCORBOT ER VII robot, 2) Human & VR games | Lumbar Postural change (Vive vs Vicon) |
| [13] | T | $d_{BS}$ = 5.40 m | $\sigma$ < 0.722 mm & < 0.278° | RMSE < 1.050 mm & < 1.124° | – | UR5 robot with Optitrack MOCAP | Tracking medical device |
| [14] | C | 90° between base stations | $\sigma$ < 0.231 mm | $\sigma$ < 0.3 mm, one active BS: $\sigma$ < 2.1mm | – | ABB-IRB 140 robot | Automated testing of industrial robot |

the pose-tracking performance and the reliability conditions within the identified upper bound, and; finally, validating the obtained results with human wrist motion trajectories.

The primary contribution of this article is the multi-level, in-depth study of the dynamic performance of VLTS. The secondary contribution is the evaluation of VLTS' precision and static pose tracking performance using standard ASTM techniques. Both contributions were made under recommended conditions for all the three VLTS devices (T, C, and HMD). Finally, the suggested approaches and guidelines will supplement the article for readers to test the performance of HTC Vive spatial tracking for their custom application by using the findings of this article.

The article is structured as follows: Section II briefs about the system used for the experiments. Section III describes the experimental scheme, rationale,and parameters considered. Section IV discusses the obtained results of precision, static and dynamic analysis of pose tracking. Section V affirms the contribution and states the probable biases of our results. Finally, the appendix describes the procedures and recommendations for customized evaluation.

## II. EXPERIMENTAL SYSTEM

### A. VIVE LIGHTHOUSE TRACKING SYSTEM

Working of VLTS is explained extensively by its developer [24]. Briefly, it is an optical navigation approach in which two base stations serve as a beacon with each one of them emitting a synchronization flash (blinking lights emitting diodes) and two infrared sweeping planes (laser beams) with two rotors spinning with constant velocity and orthogonally aligned. The tracking devices are equipped with photo-diodes and other sensors such as inertial measurement units and gyroscope to measure linear and rotational accelerations respectively. The photo-diodes detect both the signals from the base stations (infrared sweep and LED flash) to triangulate the angle between the lighthouse's normal vector and the photo-diode with the time difference. Vive's off-the-shelf algorithm fuses all these sensor data to estimate the tracked pose relative to its world frame.

### B. GROUND TRUTH SYSTEM/REFERENCE SYSTEM

The ideal candidate for a reference system (RS) to assess the VLTS for motion tracking purposes would be one of the gold standard systems in that field. Our initial testing with one such system, 'Optitrack MOCAP' resulted in poor performance of Vive even in the best case static scenario. The errors were in the range of centimeters as opposed to the millimeter range, and the jitter was high as well. This bad performance was found to be caused by the interference in infra-red bandwidth between MOCAP and VLTS. Therefore, most optical tracking systems would not serve the purpose unless the infra-red bandwidth is different. There were few workaround options

like recording the data without synchronization at different time instances, using relative measures, but these are not suitable for dynamic performance assessment.

To measure the spatial tracking performance of VLTS, especially in dynamic cases, we need a system that can be precise and reliable at high velocity and provide data with a latency $< 20$ ms [16]. An industrial serial robot meets all these criteria and, with its wide range of motion, also facilitates a meticulous study of VLTS. C16 was used as the ground truth device (shown in Fig. 1). It has a repeatability of 0.05 mm and six DOF [25]. The latency between the motion feedback frames of C16 was measured at an average of 8 ms and a maximum of 12 ms, which is well within the requirements.

**FIGURE 1.** Ground truth system: Comau NS16 1.65 foundry hand robot with the mount for controller dynamic analysis attached to the end-effector.

To mount the devices of VLTS on C16's end-effector flange (ISO9409-1-A63), customised 3D printed mounts were manufactured for each of the devices as shown in the Fig. 2.

**FIGURE 2.** Vive tracking devices with their 3D printed mounts for flange ISO9409-1-A63. From left: tracker, Controller, and HMD.

The mounts for the dynamic performance assessment are shown in Fig. 3. The two of the same tracking devices/object must be mounted on the either side of the metrology bar as recommended by the ASTM standard [23]. Metrology bar length acts as a reference quantity during analysis. In the standard's requirements, the carbon fiber material was proposed for the metrology rod so that the deflection would be less than

**FIGURE 3.** Metrology bar, with devices on both ends and its C16 tool mount. Top: A 350 mm long carbon fiber tube, with VLTS's tracker on both ends. Middle: An assembly of two carbon fiber rods and rack, with VLTS's controller on both ends. Bottom: HMD mounted on the end-effector of C16.

or equal to 0.01 mm. The tool mount and the attachments are 3D printed.

### C. CONFIGURATION OF WORK VOLUME

Here, work volume is the physical space in which the tracking system is configured. The vendor recommands a play area of $3500 \times 3500\ mm^2$ and a maximum distance between the two bases stations ($d_{BS}$) of 5000 mm. Considering the above two criteria, each base station is kept 2500 mm away from the origin of the C16 at a height of 2500 mm as shown in Fig.4. The same configuration of work volume is considered for all the evaluations.

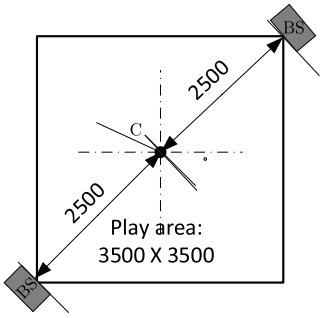


**FIGURE 4.** Work volume configuration sketch, top view. C: C16's Origin Point.

VLTS being an optics-based system, tracking performance is highly dependent on various factors such as sunlight, the presence of reflective surfaces, other IR rays interference, and visibility of photo-diodes to the base stations.

The following considerations were made within the work volume while conducting the evaluation:

- The tracking area was covered with non-reflective black sheets. All reflective objects and windows were also covered to avoid natural lights. No other infrared emitting devices were placed in the work volume (section II-C).
- Base stations were synchronized using sync cable with channel "b" and "A" with room-scale calibration
- The receiver dongle of the tracker was set 45 cm far from the computer

### D. POSE ERROR BETWEEN VLTS AND C16 ROBOT

To compare the pose of two independent systems with their own absolute frame, there are numerous techniques. The first and the most common method used in robotics is to have an intermediate frame VLTS's frame at a precisely measured point with respect to the C16's origin and transform the data using rigid body transformation. This is not suitable for performance evaluation as the system error will be reflected in each data frame. The next method, widely used in the field of computer vision since 1986, is the least square fitting technique (calibration/registration process). This has been adapted for evaluating system performance (Vicon MOCAP assessment [26]). This method requires the collection of matching data points from both the system and estimating the parameters of the rigid body transformation matrix. This topic is itself vast with solutions explored from various aspects like closed form vs iterative solution, and etc. A detailed survey and categorization of the existing methods are presented in [27] and [28]. For our experimental setup, we assessed the effectiveness of two closed-form solution algorithms [29] and [30]. Despite providing good transformation results with RMSE of 4.1 mm and 4.5 mm, we encountered a significant problem. Being a non-rigid body transformation, the outliers were also transformed i.e., the transformation includes even the deformed dataset. Thus, this method is also not suitable for our evaluation. The above-mentioned methods are used to obtain the absolute pose error in which there is a significant dependency between the two systems.

In our experimental system, as the time data are synchronized, we could evaluate the relative pose error in their own respective frame without transforming the frame from C16 to VLTS. This method fits our criteria perfectly because the error is measured without influencing either of the systems thereby removing any inter-system dependency. Let's say we have a dataset of N sample size from the C16 and VLTS. Each pose (2:N) is transformed with respect to the first pose in its own frame and then the pose error is calculated using equation (1).

$$\begin{aligned} 0 \leq e_{RelAngle,k} &= \cos^{-1}\left(\frac{trace(R_k)-1}{2}\right) < \pi \\ e_{RelTran,k} &= \sqrt{(\hat{x_k}-\hat{x_1})^2)+(\hat{y_k}-\hat{y_1})+(\hat{z_k}-\hat{z_1})^2)} \\ &\quad -\sqrt{(x_k-x_1)^2)+(y_k-y_1)+(z_k-z_1)^2)} \end{aligned} \tag{1}$$

where $e_{RelAngle,k}$ is the relative angle error, $e_{RelTran,k}$ is the relative translation error, $R_k = {}_1R_k\hat{R}_k^T$ represents the rotation difference expressed in $[3 \times 3]$ rotation matrix. The characters with $\wedge$ accent mark denotes the data measured in the coordinate frame of the VLTS, and the characters with no accent mark are data measured in the C16' coordinate frame.

### E. SYSTEM ARCHITECTURE

The architecture of the experimental setup to evaluate the VLTS is elucidated in Fig. 5. It describes the integration of two systems (C16 and VLTS) in four primary blocks. The requirement of this system is to provide pose and time data feedback synchronized in the same reference frame with a time latency of less than 22 ms.

- The role of the first block is to prepare our ground truth system C16 to perform the required motion. The trajectories are designed as specified in section III. With the use of the Universal Robot Description Format (URDF) file, the generated trajectory was simulated in MATLAB to ensure the trajectories are within the workspace. After verification, our Python PDL Parser generates the path file and send it to the C16.
- The second block is the server setup for VLTS and C16. The custom application built with OpenVR SDK (C++) [31] and WinC4G API (PDL-Comau custom scripting) acts as a server of a TCP/IP network to stream the data of VLTS and C16 respectively.
- The third block highlights the data collection software developed. The data collection API receives both the data stream in parallel, inserts the time data for synchronization, and logs it in a ".txt" file.
- The final block features the data post-processing. This process is done offline after the experimentation to reduce computation time and thereby latency while collecting the data. The stored data from both C16 and VLTS are synchronized and re-sampled at 100 Hz. Then the relative transformation and pose error are calculated as explained in section II-D. Finally, the performance metrics are evaluated.

## III. DESIGN OF EXPERIMENTS

VLTS' spatial tracking performance was tested in three cases. The first two analysis, namely precision evaluation and static analysis, were conducted with zero velocity between each data frames, and the third analysis, the dynamic analysis, examines the variation of tracking performance with different velocities. Despite comprehensive literature on precision and static analysis as illustrated in Table 1, they were undertaken for two key reasons: validating our experimental setup against the literature; and to address the variation in the literature's reports by introducing a standardized methodology and evaluation parameters. This section outlines the methods used for each type of analysis with an emphasis on the purpose, rationale, assessed criteria, and performance metrics.

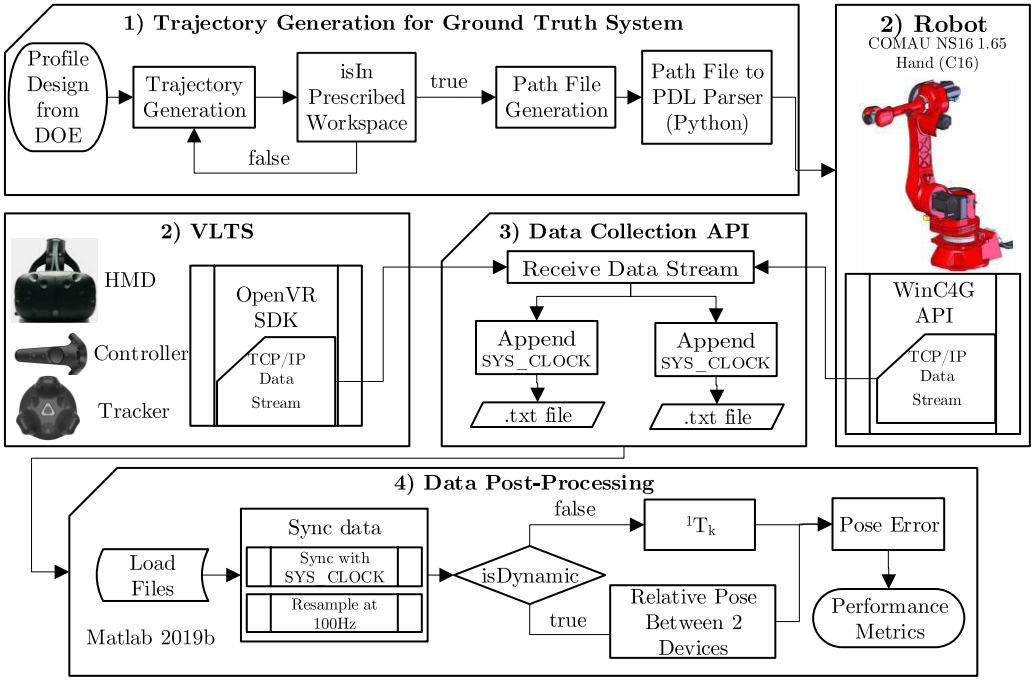


**FIGURE 5.** System architecture of the experimental setup. DOE: Design of experiments, $^1T_k$: Homogeneous transformation matrix from $k^{th}$ pose to $1^{st}$ pose. The source of the modules within the edge tapered boxes are made available in the GitHub repository [32]. The repository includes the C++ source code of the data collection API, the Python path to PDL parser script, and the MATLAB scripts developed for post-processing, transformation, generation of the performance metrics, and also for the tested registration algorithm.

### *A. PRECISION EVALUATION*

This test investigates the precision of VLTS in static case. The repeatability of the C16 (0.05 mm) allows for a precise revisit of the commanded points, which is ideal for precision evaluation. The method is as follows: the tracking device was kept at 10 random points (as shown in Fig. 6) and the data were collected for VLTS and C16. This was repeated 10 times with random order of visit. The randomness of the visits is to have ''independent test results'' [21]. The choice of 10 points and 10 visits were arbitrary. Each point's pose is evaluated 10 times leading to a total of 100 evaluations which will provide reliable data for one tracking device. The same method is followed for all three devices.

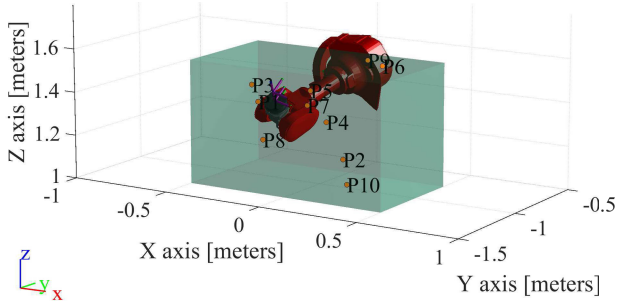


**FIGURE 6.** 10 randomly selected points (P1 to P10) within the prescribed workspace. For each iteration, the order of visit to P1 to P10 was randomly selected.

The measure of precision is generally measured in terms of imprecision and computed as standard deviations (RMSD) [21]. In addition, $d_{max}$, E(50), E(95), and E(99.7) were computed to report the quality of the pose tracking performance. $d_{max}$ indicates the largest error obtained which includes the outliers irrespective of the number of occurrences. The percentile values gives an overview of the confidence level of the pose tracking. For instance, if the 99.7 percentile value is closer to the mean value than we can infer that the pose tracking is reliable with 99.7 % confidence.

Apart from the parameter above, two statistical hypothesis tests AET and MPET were conducted. The first test was conducted to check if VLTS has an average precision of less than 1 mm and 0.5° as the literature claims(Table. 1). The latter aims to infer the maximum deviation from the mean is less than 10 mm and 1 deg. The null and alternative hypothesis are set as shown in the Table (2). The same hypothesis were tested on all the three devices of VLTS for both position and orientation.

**TABLE 2.** Statistical tests for the precision evaluation of VLTS.

| Test | Null Hypothesis | Alternative Hypothesis |
|---|---|---|
| AET | $H_0 : \bar{d} \leq \delta_{avg}$ | $H_a : \bar{d} > \delta_{avg}$ |
| MPET | $H_0 : d_{max} \leq \delta_{max}$ | $H_a : d_{max} > \delta_{max}$ |

For the average error test, the sample size is $N > 30$ and the population standard deviation is unknown, therefore the

Z-test is performed to validate the hypothesis [33]. In a statistical sense, the precision is less than $\delta_{avg}$ if the AET accepts the null hypothesis with a p-value $> 0.95$ i.e., if equation (2) is not satisfied.

$$\frac{\bar{d} - \delta_{avg}}{\sqrt{s^2/N}} > Z_\alpha \tag{2}$$

where, $Z_\alpha = 1.6449$ (Z score at 0.95).

For MPET, the null hypothesis i.e., the maximum deviation is less than 1 cm and 1° if the equation (3) is false.

$$\frac{\delta_{max} - d_{max}}{d_{max} - d_{min}} < \frac{\alpha}{1 - \alpha} \tag{3}$$

where, $\alpha = 0.05$.

### B. STATIC ANALYSIS

The static analysis is the evaluation of the system's performance when the object to be tracked and the measurement system are both static with respect to each other. This analysis is one of the most common assessment available among the literature. Each literature evaluate VLTS for their focused application and does not have a common set of metrics. There are also variation in the literature findings, some reporting millimeter accuracy while some reporting in sub-millimeter. These discrepancies are mainly due to the choice of the ground truth system, assessment techniques and evaluation methods. In this article, we aim to resolve this ambiguity by introducing a standardized method and performance evaluation metrics adapted from the ASTM standard for optical based motion tracking devices [22].

One of this standard's additional criteria is that the pose measurement uncertainty of the chosen ground truth system must be less than the measurement uncertainty associated with the test system (VLTS), which is the case of our setup with C16. The test procedure proposed by [22] is relatively straightforward. The object/device to be tracked is placed at 'N' random locations and the pose is measured simultaneously by the reference system (C16) and the system under test (VLTS). To ensure that the average error follows a normal distribution according to the central limit theorem, the number of samples (N) should be greater than 32 (N$\geq$ 32). A sample size of 100 was arbitrarily selected to provide reliable results (N=100).

Upon completion of data collection, the pose error ($e_k$) is calculated using the technique mentioned in section II-D and the equation (1). The hypothesis tests similar to section III-A were conducted with the same null and alternative hypothesis as tabulated in Table. 4 but with $\delta_{avg}$ as 5 mm and 0.5°, and $\delta_{max}$ as 10 mm and 1°. The equations (2) and (3) were used to validate the null hypothesis by replacing $\bar{d}$ with $\bar{e}$, $d_{max}$ and $d_{min}$ with $e_{max}$ and $e_{min}$.

Apart from the these two statistical tests, [22] recommends two other tests such as quantile error test and precision error test. These tests were not considered in this article because of unknown expected quantile bound value and unknown prior variance from vendor. If necessary, while performing custom evaluation, the above two tests could be conducted with the results tabulated in Table 6.

**TABLE 3.** $\delta_{avg}$ opted for dynamic analysis. $\delta_{max} = 1.5 \times \delta_{avg}$.

| Parameter | DOF | Tracker | Controller | HMD |
|---|---|---|---|---|
| $\delta_{avg}$ | P [mm] | 49.8250 | 58.5 | 97.5 |
| | O [deg] | 2 | 2 | 2 |

**TABLE 4.** Precision evaluation: Hypothesis test results.

| Device | DOF | Z value | $H_0$ | ME value | $H_0$ |
|---|---|---|---|---|---|
| T | P | -405.4498 | Accepted | 1.9061 | Accepted |
| | O | -4606.1015 | Accepted | 5.2800 | Accepted |
| C | P | -448.4230 | Accepted | 3.0316 | Accepted |
| | O | -3225.4311 | Accepted | 4.0188 | Accepted |
| HMD | P | -2077.8760 | Accepted | 12.5117 | Accepted |
| | O | -3446.2159 | Accepted | 3.8986 | Accepted |

### C. DYNAMIC ANALYSIS

The dynamic analysis focuses on the determination of the pose tracking performance of VLTS while the tracking device is in motion. As mentioned in section I, dynamic analysis is not prevalent in the literature. Here, in addition to the standard procedure from [23], we present the method to determine the performance against varying velocity and fixing the upper bound as well as verification of the results using complicated and randomized trajectories.

To avoid p-hacking [34], the entire experiment was conducted with a single goal: to study the pose tracking performance against the variation in velocity.

#### 1) STANDARD PROCEDURE EVALUATION

The standard stipulates in detail the test procedure and a set of statistically based performance metrics to evaluate the performance of an optical tracking system. The adaptation of the standard is as follows: One of the suggested test volume of $3000 \times 2000 \times 2000\ mm^3$ was configured inside our work volume of $3500 \times 3500 \times 2200\ mm^3$ (section II-C). The tracking device to be tested are attached to the ends of the metrology bar as shown in Fig. 3. The procedure requires moving the position of the centroid of the metrology bar at a relatively constant walking speed of 1500 mm/s ($1200 \pm 700$ mm/s) along the work volume in two patterns(X, Y) as shown in Fig. 7 at a height of 1000 mm.

Through a continuous smooth motion, the centroid of the metrology bar is moved along the test volume in two patterns (X and then Y) with three different orientations. The orientations are configured such that the line passing through metrology bar and the devices aligned parallel to the three orthogonal planes. Thus, for a single test a total of 6 trajectories are evaluated at the commanded average velocity.

**TABLE 5.** Precision evaluation results: Statistics on deviations from mean.

| Device | DOF | RMSD | E(50) | E(95) | E(99.7) | $\bar{d}$ | $s^2$ | $d_{max}$ |
|---|---|---|---|---|---|---|---|---|
| T | P [mm] | 0.5352 | 0.2675 | 1.0512 | 2.5625 | 0.3763 | 0.1448 | 3.4410 |
| N: 61200 | O [deg] | 0.0600 | 0.0556 | 0.0915 | 0.1374 | 0.0550 | 0.0006 | 0.1592 |
| C | P [mm] | 0.5023 | 0.2454 | 1.0285 | 2.0286 | 0.3544 | 0.1267 | 2.4804 |
| N: 61140 | O [deg] | 0.1155 | 0.1123 | 0.1585 | 0.1822 | 0.1116 | 0.0009 | 0.1993 |
| HMD | P [mm] | 0.1579 | 0.7401 | 0.3300 | 0.5243 | 0.1179 | 0.0110 | 0.873 |
| N: 61140 | O [deg] | 0.0809 | 0.0803 | 0.1161 | 0.1607 | 0.0749 | 0.0009 | 0.2041 |

**TABLE 6.** Static analysis results: Statistics on relative pose error.

| Device | DOF | RMSE | E(50) | E(95) | E(99.7) | $\bar{e}$ | $s^2$ [$mm^2$, $deg^2$] | $e_{max}$ |
|---|---|---|---|---|---|---|---|---|
| T | P [mm] | 3.3091 | 1.7581 | 6.9137 | 9.4207 | 2.5499 | 4.4482 | 9.6425 |
| N: 61185 | O [deg] | 0.5000 | 0.4638 | 0.7762 | 0.9131 | 0.4622 | 0.0364 | 0.9233 |
| C | P [mm] | 1.9826 | 1.3529 | 3.9879 | 4.7795 | 1.5963 | 1.3827 | 5.0362 |
| N: 61243 | O [deg] | 0.2494 | 0.2031 | 0.4409 | 0.5835 | 0.2210 | 0.0133 | 0.6101 |
| HMD | P [mm] | 1.5688 | 1.2313 | 2.8782 | 3.4794 | 1.3209 | 0.7165 | 3.8349 |
| N: 61140 | O [deg] | 0.2345 | 0.1657 | 0.4796 | 0.7643 | 0.1984 | 0.0156 | 0.7711 |

**TABLE 7.** ASTM, dynamic evaluation results: Statistics on pose error between the two tracking devices.

| Device | Velocity [mm/s] | DOF | RMSE | E(50) | E(95) | E(99.7) | $\bar{e}$ | $s^2$ | $e_{max}$ | %Loss |
|---|---|---|---|---|---|---|---|---|---|---|
| T | $V_{avg}$ = 885.78 | P [mm] | 562.7750 | 33.3580 | 1164.0 | 3885.248 | 201.7611 | 276053.548 | 5125.9 | 33.7829 |
| N: 6080 | $V_{max}$ = 1500.9 | O [deg] | 6.6700 | 1.5220 | 18.6890 | 27.5830 | 3.7284 | 30.5938 | 32.7830 | |
| C | $V_{avg}$ = 886.11 | P [mm] | 474.6540 | 11.8900 | 262.4120 | 3959.2 | 107.4543 | 213786.37 | 4792.4 | 11.3926 |
| N: 61185 | $V_{max}$ = 1500.9 | O [deg] | 2.9890 | 0.6560 | 6.3880 | 17.9550 | 1.4778 | 6.7493 | 21.9330 | |
| HMD | $V_{avg}$ = 902.467 | P [mm] | 48.0560 | 32.8240 | 96.7290 | 117.9570 | 38.5553 | 823.0101 | 120.6060 | 0 |
| N: 61185 | $V_{max}$ = 1501.1 | O [deg] | 1.0520 | 1.0300 | 1.6420 | 2.1480 | 0.9388 | 0.2263 | 3.7620 | |

As the relative pose between the left and right tracking devices are constant at all time, the pose measurement error is calculated by comparing ${}_{Left}\hat{H}_{Right}$ of VLTS and ${}_{Left}H_{Right}$ of C16. The timestamp is used to synchronize the data. The position error ($e_p$) and the orientation error ($e_o$) at time instance t are calculated as shown in equation 4.

$$\begin{aligned} e_p(t) &= ||\hat{T}(t)|| - ||T|| \\ e_o(t) &= \hat{\theta}(t) - 0 = \hat{\theta} \end{aligned} \tag{4}$$

where $\hat{T}(t)$ and $\hat{\theta}(t)$ are the position vector and the angle of rotation of ${}_{Left}\hat{H}_{Right}$, T is the position vector of ${}_{Left}H_{Right}$, $||\ \ ||$ denotes 2-norm of the vector. $\hat{\theta}(t)$ is calculated using the equation 5.

$$\hat{\theta}(t) = 2 * asin(\sqrt{\hat{q}_x^2(t) + \hat{q}_y^2(t) + \hat{q}_z^2(t)}) \tag{5}$$

where, $(\hat{q}_w(t), \hat{q}_x(t), \hat{q}_y(t), \hat{q}_z(t))^T$ is the unit quaternion representation of the rotation matrix $\hat{R}(t)$.

The error statistics computed are the RMSE, $e_{max}$, and the percentile error (E(99.7), E(95) and E(50)). Similar to previous section III-A and III-B, the AET and MPET hypothesis tests were performed. Here, instead of verifying the error in the millimeter or centimeter range, we intend to inspect the device in a broader perspective by examining whether the devices are able to localize itself i.e., ability to be positioned within the dimensions of the device. To this extent, we propose that the average error limit should not be outside the dimensions of the device itself on either side of the center. The half of the maximum of the three dimensions (length, breadth and height) was selected to be the expected average error limit $\delta_{avg}$ for each device as tabulated in Table. 3. The maximum error limit was selected to be $1.5 \times \ \delta_{avg}$ so that some extreme outliers are not penalized heavily. For angular DOF, an arbitrary value of 2° was chosen for $\delta_{avg}$.

This approach of fixing the $\delta_{avg}$ and $\delta_{max}$ was opted to have a general purpose results whereas the appendix demonstrates the usage of the findings presented in this article for the reader's specific application with custom $\delta_{avg}$ and $\delta_{max}$ for their intended application.

The two hypothesis test performed will not provide direct information on the loss of tracking. Therefore, we propose another parameter "Percentage loss of tracking" to determine the efficiency of tracking in dynamic cases. It was calculated as the ratio between the number of data above the $\delta_{max}$ defined for MPET and the total number of sample data collected. This parameter along with the two hypothesis tests will provide sufficient information to infer statistics on the device's performance.

### 2) DETERMINATION OF THE VELOCITY UPPER BOUND

This test is intended to determine the upper bound velocity at which the tracking is reliable and examine the performance of VLTS devices below the upper bound range. Here, we stipulate the conditions of reliable tracking as follows:

- the acceptance of null hypothesis of the AET using equation (2)
- the percentage loss of tracking must be less than 0.5% (99.5% must be accepted)

Both of these conditions are considered as the necessary condition because less error and high loss of data is not favorable and the vice-versa is also not good.

The procedure is as follows: the same set of six trajectories from ASTM test depicted in Fig. 7 is used. Here, the average velocity is reduced in steps and the results are tested for reliability at each step until the upper bound of reliable tracking is found. Then, within this bound similar procedure is followed to evaluate whether the reliability conditions holds. CDF, AET, MPET and % loss in tracking were utilized to infer statistics about the dynamic performance of the VLTS device. The same procedure was repeated for all the three devices.

### 3) SUBSTANTIATION WITH HUMAN WRIST TRAJECTORIES

The aim of this set of experiment is to validate the results inferred on the dynamic performance of VLTS in the previous section III-C2. The ideal approach would be to validate for a target application and in turn verify the usability of VLTS for that specific application. Even though the latter objective is demonstrated in the appendix, here the aim is more general. Thus, the trajectory of human wrist motion was chosen because of the likelihood of obtaining uninfluenced trajectories, not in the advantage of the performance of the device.

The ground truth trajectory profiles of generic human wrist motions were obtained using the Optitrack MOCAP equipped with 8 cameras. The MOCAP reflective markers were placed at the wrist joint centers using a wrist band as shown in Fig. 8 (left). To have more randomized and complex trajectory, the subject was advised to move his joint extremes as often as possible and no other information was provided. 8 trajectories with 3 spatial (subject was instructed to move randomly with different speed) and 5 planar motions (subject was instructed to place the palm on flat table and on a vertical board while performing motions) were recorded. The profile of the recorded trajectory was then modeled using smoothing

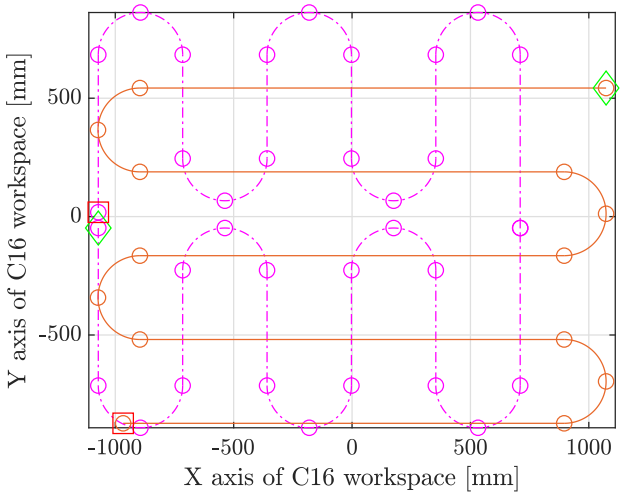


**FIGURE 7.** Pattern trajectories for dynamic analysis adapted to the C16's workspace. X pattern (horizontal lines-red) and Y pattern (vertical lines-cyan). Each pattern is parallel, straight line segments, back-and-forth along their corresponding axis with the paths separated by at most the length of the metrology bar. At maximum, one-half of the metrology bar length shall be the difference between the boundary lines and the test volume limits.

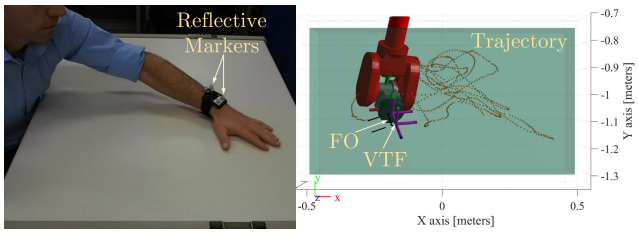


**FIGURE 8.** Left: Wrist centre of the upper arm is tracked by attaching a wrist band equipped with reflective markers. Right: the hand tracking trajectory fed to the C16, within the prescribed workspace. (FO is the offset distance of 45 millimetres where the mounting part is attached and VTF is the Vive tracker tool frame which is at distance of 19.6 millimetres from the top of the mount.

spline curve fitting with an average $R^2$ value of 0.64. The profile was transformed to fit within the prescribed workspace of the robot as shown in Fig. 8 (right) (Cuboid of 1 m x 0.55 m x 0.6 m, [35]. The workspace in which the robot can traverse linearly between any pose without hitting singularities or changing the manifold using joint space).

The difference in terms of setup between here and section II-B is the trajectory generation method for C16. For all experiments, the reference trajectories were manually generated according to requirements, but here the wrist motion of the subject was captured using Optitrack MOCAP. The sole purpose of the Optitrack MOCAP is to extract the reference trajectories from the subject which is later fitted and given as input to C16. Then, C16 was used to substantiate the VLTS's dynamic performance.

The same mount shown in Fig. 3 was used for tracker and controller. Due to practical difficulties of mounting two HMD, the single HMD mount shown in Fig. 2 (far right) was utilized. The centroid of the mounts were commanded

**TABLE 8. Velocity bound evaluation results. Statistics on pose error between the two tracking devices at the determined upper bound average velocity ($V_{avg}$).**

| Device | Velocity [mm/s] | DOF | RMSE | $e_{max}$ | E(50) | E(95) | E(99.7) | $\bar{e}$ | $s^2$ | $H_0$ | % loss |
|---|---|---|---|---|---|---|---|---|---|---|---|
| T | $V_{avg}$ = 134.6 | P [mm] | 16.6200 | 945.0550 | 2.9390 | 16.7590 | 105.1940 | 5.8020 | 242.5590 | Accepted | 0.4921 |
| N: 50722 | $V_{max}$ = 135.05 | O [deg] | 1.435 | 18.173 | 0.2810 | 1.7910 | 12.454 | 0.5838 | 1.7176 | Accepted | |
| C | $V_{avg}$ = 247.61 | P [mm] | 27.3640 | 958.4530 | 3.2320 | 14.2800 | 110.0060 | 6.0842 | 711.8 | Accepted | 0.4103 |
| N: 27296 | $V_{max}$ = 250.05 | O [deg] | 1.2860 | 26.7520 | 0.1520 | 0.8470 | 15.7730 | 0.3175 | 1.5533 | Accepted | |
| HMD | $V_{avg}$ = 853.46 | P [mm] | 47.6370 | 102.6720 | 37.8510 | 88.3020 | 102.0160 | 39.5695 | 703.6343 | Accepted | 0.0000 |
| N: 7888 | $V_{max}$ = 1000.5 | O [deg] | 1.0850 | 2.7120 | 1.0640 | 1.7290 | 2.3650 | 0.9781 | 0.2215 | Accepted | |

to follow the prepared hand trajectory profiles. The error was calculated using the equation (4) for tracker and controller and equation (1) for HMD. Each trajectory's tracking data was examined for reliability and the corresponding velocity is verified against the upper bound reported by previous section III-C2.

## IV. RESULTS AND DISCUSSION

This section will discuss the significant observations made from the data obtained during the experimentation.

### A. PRECISION EVALUATION

The precision evaluation was conducted as per the methodology mentioned in section III-A, the measure of precision along with the other parameters to access the quality of tracking was computed, and tabulated in the Table 5. It can be observed that all the three devices demonstrated high precision with RMSD less than 0.55 mm and 0.12°.

From the CDF shown in Fig. 9a, it is evident that HMD has an excellent precision with the peak value of 0.74 mm. Tracker and controller tracked 94.155% and 94.578% of data within 1 mm. For the angular DOF shown in Fig. 9b, tracker oriented 97.259% of the sample within 0.1° precision. HMD and Controller tracked 78.471% and 0.333% within 0.1°. The worst deviation of 2.5625 mm at 99.7 percentile further confirms the excellent results obtained with VLTS on the overall quality of the static spatial tracking precision.

Using the value of $\bar{d}$ and $s^2$ in the Table. 5, the hypothesis tests were conducted and the results are tabulated in the Table. 4. All the $H_0$ was accepted. Thus, we can statistically infer the following for of all the three VLTS devices:

- The average deviation from mean is in sub-millimeter ( $< 1$ mm ) and less than 0.5°.
- The maximum deviation from mean is less than 10 mm and 1°.

### B. STATIC ANALYSIS

The results of the static analysis conducted using the standard procedure explained in section III-B are tabulated in the Table. 6. The RMSE was found to be in the millimeter range rather than the sub-millimeter range of some literature. From the CDF of the position and orientation error shown in Fig. 9c and Fig. 9d, it can be seen that the HMD tracked with 96.44% and 98.99% of the sample within 3 mm and 0.5°, controller's 85.61% and 95.48% of data has error below 3 mm and 0.5° whereas for the same error value, tracker has 67.04% and 51.56%.

**TABLE 9. Static analysis: Hypothesis test results.**

| Device | DOF | Z value | $H_0$ | ME value | $H_0$ |
|---|---|---|---|---|---|
| T | P | -40.8321 | Accepted | 0.0371 | *Rejected* |
| | O | -37.9068 | Accepted | 0.0831 | Accepted |
| C | P | -295.4226 | Accepted | 0.9856 | Accepted |
| | O | -597.7264 | Accepted | 0.6390 | Accepted |
| HMD | P | -490.6218 | Accepted | 1.6076 | Accepted |
| | O | -596.5022 | Accepted | 0.2968 | Accepted |

The outcomes of the hypothesis tests are tabulated in Table. 9 with their corresponding test scores (Z value: Result of the AET in equation (2), ME value: Result of the MPET in equation (3)). All the null hypothesis was satisfied except for the liner DOF of the tracker device, the maximum permissible error's hypothesis was rejected. Upon further analysis, the maximum permissible positional error of the tracker was identified to be less than 11 mm. Thus in a statistical sense, we can infer the following on the static performance (accuracy) of the three VLTS devices:

1) The average pose error is less than 3 mm and 0.5°
2) The maximum pose error is less than 11 mm and 1°

### C. DYNAMIC ANALYSIS

#### 1) STANDARD ASTM PROCEDURE

Table. 7 presents the results of the standard procedure evaluation of the VLTS's dynamic analysis as mentioned in section III-C. The average velocity of the trajectory during the test was 902.467 mm/s and a maximum of 1501.1 mm/s which confines with the recommendations of the standard. This velocity is approximately 15 times higher than the literature (60 mm/s). The tracking performance was highly poor which is clear from the CDF of the error (using equation (4) until $\delta_{max}$) shown in Fig. 9e and 9f. It was observed that only 18.7007 %, 44.3802 %, and 17.5275 % of data is less than 10 mm error and 61.5296%, 81.2617%, and 91.4467% of data

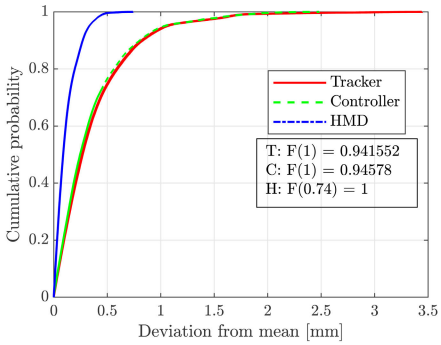


(a) Precision evaluation: CDF of positional deviation from mean.

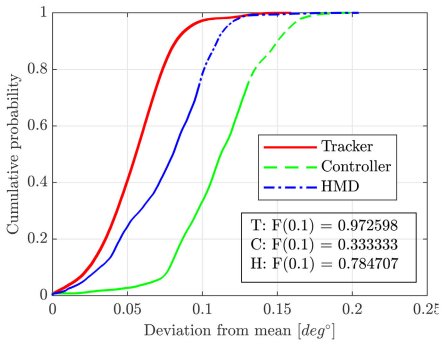


(b) Precision evaluation: CDF of orientation deviation from mean.

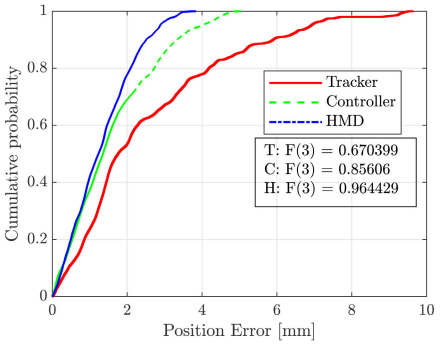


(c) Static analysis: CDF of position error.

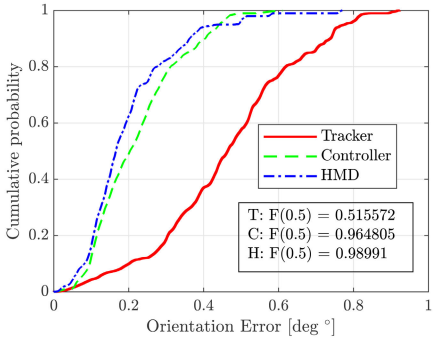


(d) Static analysis: CDF of orientation error.

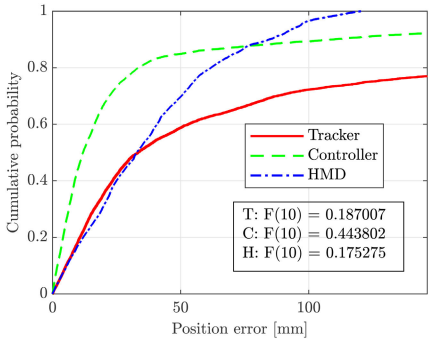


(e) Dynamic evaluation: CDF of position error (up to 146.5 mm).

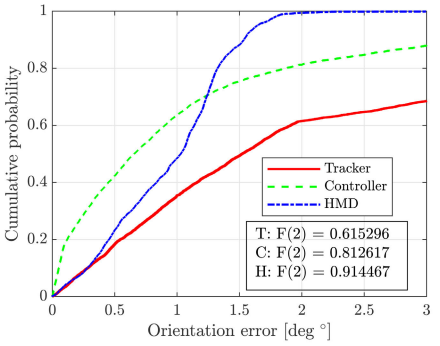


(f) Dynamic evaluation: CDF of orientation error ( up to 3°).

**FIGURE 9.** ASTM Standard evaluation results: CDF of position and orientation error for precision evaluation, static analysis, and standard dynamic analysis.

**TABLE 10.** ASTM, dynamic evaluation: Hypothesis test results.

| Device | DOF | Z value | $H_0$ | ME value | $H_0$ |
|---|---|---|---|---|---|
| T | P | 22.5484 | *Rejected* | -0.9854 | *Rejected* |
| | O | 24.3661 | *Rejected* | -0.9085 | *Rejected* |
| C | P | 8.1194 | *Rejected* | -0.9817 | *Rejected* |
| | O | -15.4156 | Accepted | -0.8632 | *Rejected* |
| HMD | P | -177.6190 | Accepted | 0.2126 | Accepted |
| | O | -164.2445 | Accepted | -0.2026 | *Rejected* |

is less than 2° of orientation error for tracker, controller, and HMD respectively.

The hypothesis test's outcome tabulated in Table. 10 shows that except the HMD's positional performance all other null hypothesis were rejected.

The % loss of tracking computed, further asserts that all devices have poor spatial tracking performance except for the positional tracking of HMD. Since the standard procedure did not provide any significant insight on the dynamic performance capabilities of VLTS, we continue to analyze the devices using the same trajectories of this test but with lower average velocity ($< 902.467$ mm/s).

### 2) DETERMINATION OF THE VELOCITY UPPER BOUND

The VLTS was evaluated for reliability under reduced average velocity of the trajectories. The conditions of reliability (III-C2) was evaluated at each step gradually with reduced average velocity through interval analysis and the results are summarized in detail in the appendix Table 14 for the tracker, controller and HMD.

Both the reliability conditions were found to be satisfied at an average velocity of 134.6 mm/s, 240.61 mm/s, and 853.46 mm/s for tracker, controller, and HMD respectively. The results at the reliable velocity is tabulated in Table 8. At this upper bound, the devices were able to localize within itself without loss of tracking.

HMD's superior results are due to many factors, but the significant factor is that the number of photo-diodes is higher than the other two devices.

From the CDFs of position and orientation error shown in Fig. 10 (for the trajectories less than the determined upper bound), we can observe that the curve signifies a good performance for all the devices i.e, within the bound the devices are able to localize themselves without losing more than 99.5% of data. Therefore from this analysis, we can infer the following on the upper bound of VLTS:

- The reliable upper bound velocity of the VLTS devices are 134.6 mm/s (Tracker), 240.61 mm/s (Controller), and 853.46 mm/s (HMD) with
  - the average error is less than the $\delta_{avg}$ (Refer Table. 3) and
  - the maximum error is less than the $\delta_{max}$ ($= 1.5 \times \delta_{avg}$)

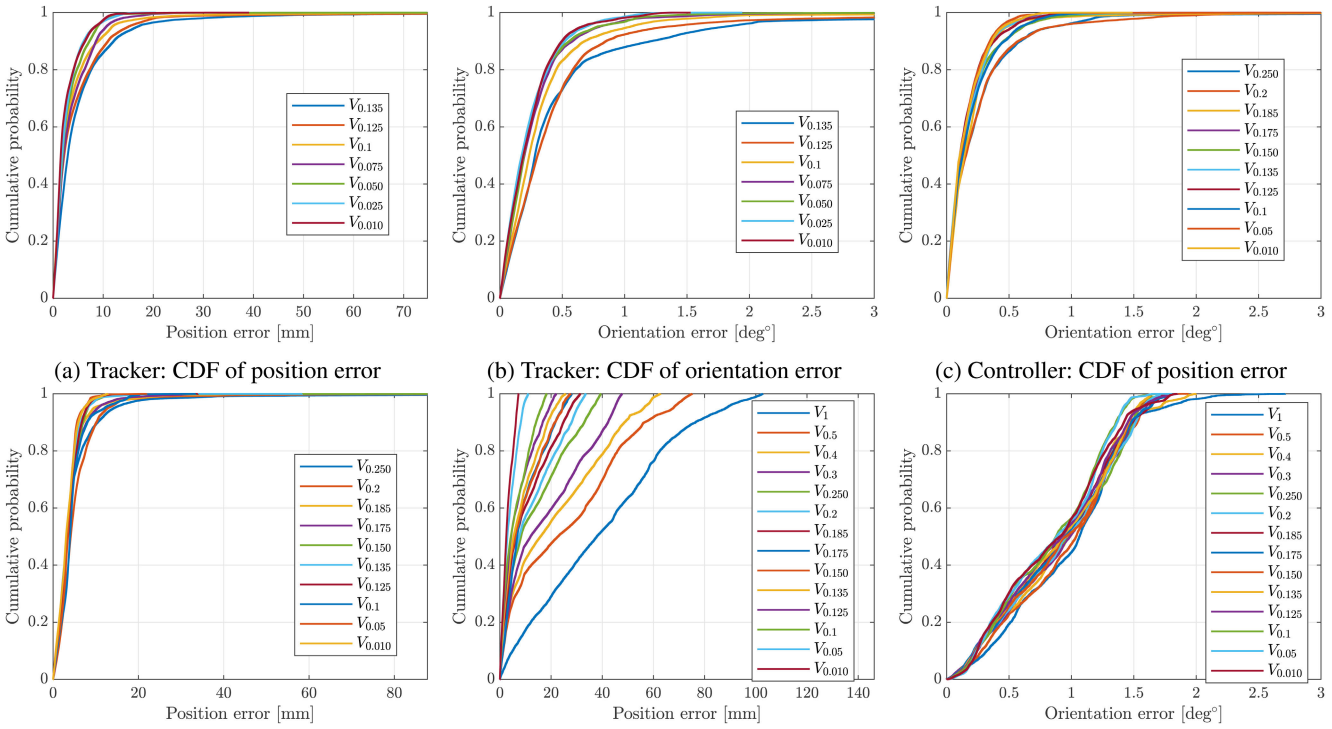


(a) Tracker: CDF of position error (b) Tracker: CDF of orientation error (c) Controller: CDF of position error

(d) Controller: CDF of orientation error (e) HMD: CDF of position error (f) HMD: CDF of orientation error

**FIGURE 10.** Velocity bound evaluation: CDF of position and orientation error up to $\delta_{max}$ for tests with velocities less than the upper bound.

**TABLE 11.** Wrist trajectory evaluation results, Tracker: Statistics on pose error between the two tracking devices.

| Traj./ N | Velocity [mm/s] | DOF | RMSE | $e_{max}$ | E(50) | E(95) | E(99.7) | $\bar{e}$ | $AE : H_0$ | $MPE : H_0$ | % loss |
|---|---|---|---|---|---|---|---|---|---|---|---|
| S1 | $V_{avg}$ = 28.16 | P [mm] | 3.7110 | 24.7980 | 2.5200 | 7.0830 | 17.1220 | 2.8081 | Accepted | Accepted | 0.0000 |
| N: 35178 | $V_{max}$ = 35.64 | O [deg] | 0.2530 | 0.7810 | 0.2050 | 0.4250 | 0.7670 | 0.2179 | Accepted | Accepted | |
| S2 | $V_{avg}$ = 48.92 | P [mm] | 3.3600 | 25.1800 | 1.9240 | 5.9430 | 17.6860 | 2.4470 | Accepted | Accepted | 0.0000 |
| N: 63875 | $V_{max}$ = 103.30 | O [deg] | 0.1990 | 0.8750 | 0.1480 | 0.3600 | 0.7660 | 0.1619 | Accepted | Accepted | |
| S3 | $V_{avg}$ = 45.58 | P [mm] | 3.0010 | 23.9530 | 1.6310 | 4.3860 | 18.9690 | 2.0075 | Accepted | Accepted | 0.0000 |
| N: 55652 | $V_{max}$ = 65.37 | O [deg] | 0.2250 | 0.8120 | 0.1720 | 0.4180 | 0.6640 | 0.1880 | Accepted | Accepted | |
| P1 | $V_{avg}$ = 18.21 | P [mm] | 4.8560 | 23.1790 | 2.5040 | 10.8960 | 20.5500 | 3.2866 | Accepted | Accepted | 0.0000 |
| N: 23197 | $V_{max}$ = 37.55 | O [deg] | 0.3590 | 0.7620 | 0.3430 | 0.5260 | 0.6570 | 0.3308 | Accepted | Accepted | |
| P2 | $V_{avg}$ = 51.20 | P [mm] | 3.1850 | 24.0930 | 1.4490 | 6.9270 | 17.9490 | 2.0550 | Accepted | Accepted | 0.0000 |
| N: 70671 | $V_{max}$ = 100.13 | O [deg] | 0.2480 | 0.9410 | 0.1950 | 0.4220 | 0.8740 | 0.2105 | Accepted | Accepted | |
| P3 | $V_{avg}$ = 166.67 | P [mm] | 37.31 | 220.26 | 13.6650 | 80.6990 | 209.4960 | 23.1034 | Accepted | *Rejected* | 6.4561 |
| N: 11493 | $V_{max}$ = 177.82 | O [deg] | 0.9230 | 8.0430 | 0.6130 | 1.7830 | 4.4720 | 0.7150 | Accepted | *Rejected* | |
| P4 | $V_{avg}$ = 37.38 | P [mm] | 6.0720 | 40.7720 | 3.4810 | 11.7670 | 28.2770 | 4.6310 | Accepted | Accepted | 0.0000 |
| N: 47072 | $V_{max}$ = 74.32 | O [deg] | 0.4600 | 1.3340 | 0.1860 | 1.0140 | 1.2590 | 0.3214 | Accepted | Accepted | |
| P5 | $V_{avg}$ = 34.60 | P [mm] | 3.3400 | 27.8030 | 1.1880 | 6.1030 | 20.5790 | 1.9056 | Accepted | Accepted | 0.0000 |
| N: 153963 | $V_{max}$ = 35.57 | O [deg] | 0.2340 | 0.9600 | 0.1950 | 0.4000 | 0.7430 | 0.2041 | Accepted | Accepted | |

An overview of the performance is shown in Fig. 11 in terms of overall percentage of loss at different range of velocities computed for all the trajectories (i.e., each error and its corresponding velocity was extracted from all the trajectory data). It can be clearly noticed that the above 300 mm/s the tracker suffers a significant loss of data (> 10%) and the same can be observed for controller at velocity above 600 mm/s.

**TABLE 12.** Wrist trajectory evaluation results, Controller: Statistics on pose error between the two tracking devices.

| Traj./ N | Velocity [mm/s] | DOF | RMSE | $e_{max}$ | E(50) | E(95) | E(99.7) | $\bar{e}$ | $AE : H_0$ | $MPE : H_0$ | % loss |
|---|---|---|---|---|---|---|---|---|---|---|---|
| S1 | $V_{avg}$ = 141.14 | P [mm] | 6.6130 | 24.2870 | 2.5970 | 20.8640 | 23.4870 | 4.1901 | Accepted | Accepted | 0.0000 |
| N: 6441 | $V_{max}$ = 177.96 | O [deg] | 0.2080 | 1.1990 | 0.0470 | 0.4710 | 1.1700 | 0.1016 | Accepted | Accepted | |
| S2 | $V_{avg}$ = 244.82 | P [mm] | 11.6700 | 89.4040 | 1.9400 | 22.9620 | 74.0030 | 5.2973 | Accepted | *Rejected* | 0.0079 |
| N: 12643 | $V_{max}$ = 510.93 | O [deg] | 0.9040 | 5.9710 | 0.3110 | 1.4790 | 4.9540 | 0.5348 | Accepted | *Rejected* | |
| S3 | $V_{avg}$ = 229.15 | P [mm] | 1.5620 | 4.4510 | 1.0800 | 3.0050 | 4.0030 | 1.2520 | Accepted | Accepted | 0.0000 |
| N: 11015 | $V_{max}$ = 326.51 | O [deg] | 0.2090 | 0.5270 | 0.1680 | 0.3700 | 0.4840 | 0.1808 | Accepted | Accepted | |
| P1 | $V_{avg}$ = 90.95 | P [mm] | 2.0910 | 3.6320 | 2.1080 | 2.8170 | 3.2500 | 2.0023 | Accepted | Accepted | 0.0000 |
| N: 4561 | $V_{max}$ = 182.12 | O [deg] | 0.0720 | 0.3230 | 0.0470 | 0.1390 | 0.2920 | 0.0543 | Accepted | Accepted | |
| P2 | $V_{avg}$ = 256.89 | P [mm] | 37.45 | 1014.2 | 4.3700 | 40.8050 | 283.9240 | 14.3968 | Accepted | *Rejected* | 3.3506 |
| N: 14022 | $V_{max}$ = 500.61 | O [deg] | 1.0050 | 10.9920 | 0.2400 | 1.7550 | 6.5910 | 0.5308 | Accepted | *Rejected* | |
| P3 | $V_{avg}$ = 139.93 | P [mm] | 1.3290 | 6.8520 | 0.9680 | 2.5090 | 4.0580 | 1.0826 | Accepted | Accepted | 0.0000 |
| N: 14296 | $V_{max}$ = 177.83 | O [deg] | 0.0850 | 0.3660 | 0.0570 | 0.1780 | 0.2880 | 0.0662 | Accepted | Accepted | |
| P4 | $V_{avg}$ = 187.59 | P [mm] | 1.0040 | 2.5660 | 0.8410 | 1.8030 | 2.2580 | 0.8541 | Accepted | Accepted | 0.0000 |
| N: 9256 | $V_{max}$ = 364.21 | O [deg] | 0.2740 | 0.5410 | 0.2540 | 0.3960 | 0.5120 | 0.2632 | Accepted | Accepted | |

**TABLE 13.** Wrist Trajectory evaluation results, HMD: Statistics on pose error.

| Traj./ N | Velocity [mm/s] | DOF | RMSE | $e_{max}$ | E(50) | E(95) | E(99.7) | $\bar{e}$ | $AE : H_0$ | $MPE : H_0$ | % loss |
|---|---|---|---|---|---|---|---|---|---|---|---|
| S1 | $V_{avg}$ = 140.99 | P [mm] | 7.5920 | 17.9790 | 4.9410 | 14.9110 | 17.1250 | 6.0573 | Accepted | Accepted | 0.0000 |
| N: 6837 | $V_{max}$ = 177.91 | O [deg] | 0.3030 | 0.5800 | 0.2750 | 0.4870 | 0.5710 | 0.2721 | Accepted | Accepted | |
| P2 | $V_{avg}$ = 256.55 | P [mm] | 15.5820 | 36.7460 | 11.0070 | 30.4170 | 34.9950 | 12.7158 | Accepted | Accepted | 0.0000 |
| N: 14030 | $V_{max}$ = 500.61 | O [deg] | 0.1900 | 0.5090 | 0.1600 | 0.3140 | 0.4710 | 0.1690 | Accepted | Accepted | |
| P5 | $V_{avg}$ = 172.89 | P [mm] | 7.8260 | 17.0940 | 6.5230 | 13.4010 | 15.7050 | 6.6888 | Accepted | Accepted | 0.0000 |
| N: 30815 | $V_{max}$ = 177.66 | O [deg] | 0.1900 | 0.4050 | 0.1810 | 0.2760 | 0.3420 | 0.1801 | Accepted | Accepted | |

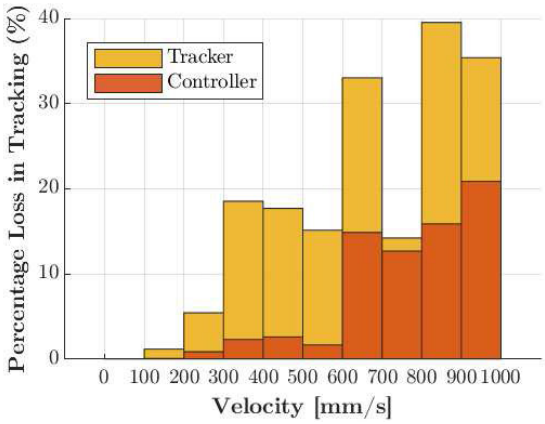


**FIGURE 11.** Overall percentage loss in tracking for tracker and controller (14 sets * 6 subsets, a total of 84 trajectories for tracker and controller) and percentage of loss was calculated over a range of 0 to 1000 mm/s in 10 steps).

A detailed results are tabulated in the appendix Table 14 which includes performance parameter such as RMSE, percentile error, $\bar{e}$, $s^2$, $e_{max}$ for both position and orientation. This table has two key significance: first, as defined in the appendix A and B, the user may utilize the value of the parameters in the table to calibrate and configure their VLTS for a particular application. Secondly, to evaluate the usability of VLTS devices for the required average velocity, the reader could simply use the tables as a look-up table/guide, so that the reader could choose to calibrate further using the techniques discussed in this article or add a filter to eliminate the measurement uncertainty using the tables' data.

### 3) SUBSTANTIATION WITH HUMAN WRIST TRAJECTORIES

The devices were tracked while performing the fitted human wrist profiles as explained in section III-C3 and the results are displayed in Table. 11, 12, and 13 for tracker, controller, and HMD correspondingly. Similar performance parameters were calculated like other evaluations especially RMSE, percentile error, hypothesis test and % loss. The reliability conditions were investigated on each profile and the non-reliable data was verified against the upper bound reported in section IV-C2. For the HMD, as the upper bound was high, all the trajectories tracked were found reliable so only three trajectories results are shown in the Table 13. For the tracker,

**TABLE 14.** Velocity bound evaluation results, Highlighted (gray) row corresponds to the identified upper bound.

| Velocity [mm/s] | N | DOF | RMSE | $e_{max}$ | E(50) | E(95) | E(99.7) | $\bar{e}$ | $s^2$ | $H_0$ | % loss |
|---|---|---|---|---|---|---|---|---|---|---|---|
| Tracker: Statistics on pose error between the two tracking devices. | | | | | | | | | | | |
| $V_{avg}$ = 844.72 | 6053 | P [mm] | 363.1460 | 3792.64 | 36.8620 | 487.5710 | 3268.269 | 124.7633 | 116328.1 | *Rejected* | 33.7519 |
| $V_{max}$ = 1000.5 | | O [deg] | 7.4080 | 35.3360 | 1.6210 | 18.3830 | 33.7170 | 4.1969 | 37.2708 | *Rejected* | |
| $V_{avg}$ = 484.01 | 12826 | P [mm] | 343.1530 | 4815.7 | 12.8390 | 306.5680 | 3633.8 | 81.6145 | 111101.9 | *Rejected* | 15.6401 |
| $V_{max}$ = 500.76 | | O [deg] | 4.8590 | 40.0370 | 0.9480 | 12.9760 | 23.3790 | 2.4616 | 17.5550 | *Rejected* | |
| $V_{avg}$ = 247.59 | 27082 | P [mm] | 298.7720 | 4899.3 | 5.8480 | 103.7330 | 3526.2 | 44.8902 | 87252.6 | Accepted | 7.4551 |
| $V_{max}$ = 250.05 | | O [deg] | 3.001 | 38.6600 | 0.4850 | 5.4820 | 19.8450 | 1.2617 | 7.4129 | Accepted | |
| $V_{avg}$ = 198.67 | 33751 | P [mm] | 133.2400 | 2382.1 | 4.8110 | 43.6040 | 1512.7 | 20.8 | 17321.0 | Accepted | 2.2547 |
| $V_{max}$ = 200.1 | | O [deg] | 2.6480 | 32.9840 | 0.3490 | 2.6060 | 27.4300 | 0.8909 | 6.2182 | Accepted | |
| $V_{avg}$ = 183.94 | 36430 | P [mm] | 75.377 | 2248.1 | 4.305 | 40.4790 | 402.639 | 14.3781 | 5475.1 | Accepted | 2.3936 |
| $V_{max}$ = 185.13 | | O [deg] | 4.0520 | 37.2820 | 0.3660 | 6.3950 | 27.515 | 1.3769 | 14.5273 | Accepted | |
| $V_{avg}$ = 174.10 | 38649 | P [mm] | 31.9130 | 431.181 | 3.8560 | 31.9030 | 270.2170 | 10.776 | 902.3714 | Accepted | 2.3105 |
| $V_{max}$ = 175.13 | | O [deg] | 1.7520 | 24.1030 | 0.356 | 2.3950 | 15.2680 | 0.7485 | 2.5103 | Accepted | |
| $V_{avg}$ = 149.42 | 45571 | P [mm] | 24.9910 | 911.09 | 3.059 | 26.7650 | 133.419 | 7.7316 | 564.787 | Accepted | 1.0116 |
| $V_{max}$ = 150.08 | | O [deg] | 1.0470 | 11.446 | 0.3120 | 2.011 | 6.7270 | 0.5854 | 0.7527 | Accepted | |
| $V_{avg}$ = 134.6 | 50722 | P [mm] | 16.6200 | 945.0550 | 2.9390 | 16.7590 | 105.1940 | 5.8020 | 242.5590 | Accepted | 0.4921 |
| $V_{max}$ = 135.05 | | O [deg] | 1.435 | 18.173 | 0.2810 | 1.7910 | 12.454 | 0.5838 | 1.7176 | Accepted | |
| $V_{avg}$ = 124.65 | 54706 | P [mm] | 13.8740 | 496.368 | 2.225 | 14.954 | 104.22 | 4.9429 | 167.7522 | Accepted | 0.4424 |
| $V_{max}$ = 125.04 | | O [deg] | 1.5290 | 28.463 | 0.302 | 1.321 | 11.666 | 0.5243 | 1.7659 | Accepted | |
| $V_{avg}$ = 99.84 | 68817 | P [mm] | 8.8470 | 252.564 | 2.051 | 11.749 | 57.694 | 3.9 | 63.0563 | Accepted | 0.1410 |
| $V_{max}$ = 100.07 | | O [deg] | 0.659 | 17.31 | 0.235 | 1.041 | 4.330 | 0.3495 | 0.3122 | Accepted | |
| $V_{avg}$ = 74.94 | 92038 | P [mm] | 5.2970 | 98.947 | 2.104 | 10.5810 | 22.451 | 3.5604 | 15.3867 | Accepted | 0.0109 |
| $V_{max}$ = 75.05 | | O [deg] | 0.423 | 10.7250 | 0.197 | 0.794 | 2.293 | 0.2779 | 0.1017 | Accepted | |
| $V_{avg}$ = 49.98 | 139926 | P [mm] | 4.4770 | 197.92 | 1.915 | 8.839 | 18.897 | 2.955 | 11.3111 | Accepted | 0.0079 |
| $V_{max}$ = 50.05 | | O [deg] | 0.3930 | 8.4180 | 0.1930 | 0.777 | 1.915 | 0.2653 | 0.0837 | Accepted | |
| $V_{avg}$ = 24.99 | 281257 | P [mm] | 3.796 | 20.513 | 1.818 | 8.323 | 14.685 | 2.7066 | 7.081 | Accepted | 0.0000 |
| $V_{max}$ = 25.06 | | O [deg] | 0.324 | 1.9430 | 0.175 | 0.686 | 1.199 | 0.2369 | 0.0485 | Accepted | |
| $V_{avg}$ = 9.99 | 704694 | P [mm] | 3.721 | 39.132 | 1.527 | 8.336 | 15.438 | 2.5553 | 7.3185 | Accepted | 0.0000 |
| $V_{max}$ = 10.05 | | O [deg] | 0.328 | 1.529 | 0.188 | 0.653 | 1.252 | 0.2413 | 0.0492 | Accepted | |
| Controller: Statistics on pose error between the two tracking devices. | | | | | | | | | | | |
| $V_{avg}$ = 843.20 | 6441 | P [mm] | 439.1060 | 4264.01 | 12.7170 | 962.2650 | 2756.7 | 136.7504 | 174140.5 | *Rejected* | 16.0534 |
| $V_{max}$ = 1000.5 | | O [deg] | 4.8320 | 30.6040 | 1.0330 | 10.2410 | 29.6960 | 2.3345 | 17.9006 | *Rejected* | |
| $V_{avg}$ = 484.45 | 13029 | P [mm] | 249.9880 | 5375.2 | 5.4090 | 37.7980 | 2779.7 | 29.4976 | 61628.86 | Accepted | 2.1414 |
| $V_{max}$ = 500.75 | | O [deg] | 1.0270 | 7.6570 | 0.1850 | 1.8140 | 6.8960 | 0.4616 | 0.8424 | Accepted | |
| $V_{avg}$ = 389.17 | 17235 | P [mm] | 101.3760 | 1825.6 | 4.8870 | 28.4040 | 1186.9 | 16.9618 | 9990.0 | Accepted | 1.4331 |
| $V_{max}$ = 400.46 | | O [deg] | 0.7010 | 10.2600 | 0.2180 | 1.3490 | 4.2380 | 0.4041 | 0.3276 | Accepted | |
| $V_{avg}$ = 295.02 | 22746 | P [mm] | 46.1490 | 1547.3 | 4.9230 | 52.6810 | 366.7620 | 13.9838 | 1934.3 | Accepted | 3.4204 |
| $V_{max}$ = 300.11 | | O [deg] | 0.8980 | 18.9910 | 0.2320 | 1.3670 | 4.2910 | 0.4070 | 0.6409 | Accepted | |
| $V_{avg}$ = 247.61 | 27296 | P [mm] | 27.3640 | 958.4530 | 3.2320 | 14.2800 | 110.0060 | 6.0842 | 711.8 | Accepted | 0.4103 |
| $V_{max}$ = 250.05 | | O [deg] | 1.2860 | 26.7520 | 0.1520 | 0.8470 | 15.7730 | 0.3175 | 1.5533 | Accepted | |
| $V_{avg}$ = 198.67 | 33857 | P [mm] | 10.2180 | 287.3180 | 4.1360 | 12.8330 | 60.8330 | 5.5801 | 73.2805 | Accepted | 0.2068 |
| $V_{max}$ = 200.10 | | O [deg] | 0.500 | 12.9080 | 0.1550 | 0.8450 | 2.8750 | 0.2677 | 0.1779 | Accepted | |
| $V_{avg}$ = 183.68 | 37258 | P [mm] | 8.2430 | 246.5230 | 3.4270 | 9.5630 | 39.2110 | 4.2109 | 50.2173 | Accepted | 0.1476 |
| $V_{max}$ = 185.13 | | O [deg] | 0.3490 | 7.1770 | 0.1430 | 0.4810 | 2.4860 | 0.1987 | 0.0826 | Accepted | |

**TABLE 14.** *(Continued.)* **Velocity bound evaluation results, Highlighted (gray) row corresponds to the identified upper bound.**

| | | | | | | | | | | | |
|---|---|---|---|---|---|---|---|---|---|---|---|
| $V_{avg}$ = 174.11 | 38985 | P [mm] | 7.4530 | 193.0960 | 3.4540 | 10.4670 | 321.0320 | 4.3891 | 36.2829 | Accepted | 0.1052 |
| $V_{max}$ = 175.13 | | O [deg] | 0.2500 | 5.6870 | 0.1130 | 0.4630 | 1.4900 | 0.1668 | 0.0348 | Accepted | |
| $V_{avg}$ = 149.29 | 45844 | P [mm] | 5.3220 | 156.6310 | 3.5110 | 8.1610 | 16.7300 | 3.8603 | 13.4194 | Accepted | 0.0349 |
| $V_{max}$ = 150.08 | | O [deg] | 0.2940 | 5.6380 | 0.1250 | 0.6100 | 1.3910 | 0.1941 | 0.0488 | Accepted | |
| $V_{avg}$ = 134.49 | 51269 | P [mm] | 4.6100 | 58.3530 | 3.4160 | 8.0790 | 19.9560 | 3.7402 | 7.2628 | Accepted | 0.0000 |
| $V_{max}$ = 135.05 | | O [deg] | 0.2510 | 3.7700 | 0.1100 | 0.4710 | 1.2810 | 0.1703 | 0.0339 | Accepted | |
| $V_{avg}$ = 124.65 | 51466 | P [mm] | 4.5010 | 33.9030 | 3.4980 | 7.8780 | 13.4430 | 3.7365 | 6.2982 | Accepted | 0.0000 |
| $V_{max}$ = 125.04 | | O [deg] | 0.2410 | 7.4890 | 0.1050 | 0.5310 | 1.0330 | 0.1632 | 0.0312 | Accepted | |
| $V_{avg}$ = 99.78 | 69266 | P [mm] | 5.7420 | 33.3940 | 3.9850 | 12.0900 | 20.2540 | 4.5338 | 12.4136 | Accepted | 0.0000 |
| $V_{max}$ = 100.07 | | O [deg] | 0.2720 | 1.4240 | 0.1280 | 0.5910 | 1.0600 | 0.1910 | 0.0373 | Accepted | |
| $V_{avg}$ = 49.97 | 140318 | P [mm] | 4.0820 | 21.9090 | 3.4330 | 7.2730 | 11.9960 | 3.5062 | 4.3658 | Accepted | 0.0000 |
| $V_{max}$ = 50.05 | | O [deg] | 0.2180 | 3.5390 | 0.1100 | 0.4320 | 0.7540 | 0.1560 | 0.0231 | Accepted | |
| $V_{avg}$ = 9.99 | 704464 | P [mm] | 4.0060 | 12.8560 | 3.0400 | 7.2370 | 12.3260 | 3.3431 | 4.8697 | Accepted | 0.0000 |
| $V_{max}$ = 10.05 | | O [deg] | 0.2170 | 1.4910 | 0.1050 | 0.4520 | 0.7460 | 0.1581 | 0.0220 | Accepted | |
| HMD: Statistics on relative pose error. | | | | | | | | | | | |
| $V_{avg}$ = 853.46 | 7888 | P [mm] | 47.6370 | 102.6720 | 37.8510 | 88.3020 | 102.0160 | 39.5695 | 703.6343 | Accepted | 0.0000 |
| $V_{max}$ = 1000.5 | | O [deg] | 1.0850 | 2.7120 | 1.0640 | 1.7290 | 2.3650 | 0.9781 | 0.2215 | Accepted | |
| $V_{avg}$ = 484.55 | 13688 | P [mm] | 33.9810 | 75.1200 | 22.6520 | 67.7220 | 74.4880 | 26.0019 | 478.6289 | Accepted | 0.0000 |
| $V_{max}$ = 500.75 | | O [deg] | 1.0510 | 1.9390 | 1.0370 | 1.5700 | 1.7590 | 0.9477 | 0.2064 | Accepted | |
| $V_{avg}$ = 391.01 | 17545 | P [mm] | 28.1050 | 62.7540 | 15.8370 | 56.2230 | 62.1240 | 21.0501 | 346.8232 | Accepted | 0.0000 |
| $V_{max}$ = 400.47 | | O [deg] | 1.0330 | 1.9990 | 0.9830 | 1.6630 | 1.9650 | 0.9195 | 0.2223 | Accepted | |
| $V_{avg}$ = 295.80 | 26865 | P [mm] | 23.3250 | 47.7350 | 11.9690 | 44.7850 | 47.5080 | 17.5017 | 237.7740 | Accepted | 0.0000 |
| $V_{max}$ = 300.11 | | O [deg] | 1.0330 | 1.8490 | 0.9880 | 1.5910 | 1.8030 | 0.9207 | 0.2190 | Accepted | |
| $V_{avg}$ = 247.46 | 27665 | P [mm] | 17.6780 | 39.4800 | 8.2700 | 36.0390 | 39.2580 | 12.9919 | 143.7414 | Accepted | 0.0000 |
| $V_{max}$ = 250.04 | | O [deg] | 1.0250 | 1.8300 | 0.9590 | 1.5470 | 1.7540 | 0.9079 | 0.2258 | Accepted | |
| $V_{avg}$ = 198.67 | 34865 | P [mm] | 15.1350 | 33.6590 | 7.5740 | 30.2380 | 33.3580 | 11.2635 | 102.2142 | Accepted | 0.0000 |
| $V_{max}$ = 200.10 | | O [deg] | 1.0290 | 1.7390 | 0.9580 | 1.5740 | 1.7070 | 0.9157 | 0.2196 | Accepted | |
| $V_{avg}$ = 183.96 | 38166 | P [mm] | 13.4940 | 31.4470 | 6.3680 | 27.6240 | 31.1830 | 9.9602 | 82.8907 | Accepted | 0.0000 |
| $V_{max}$ = 185.13 | | O [deg] | 1.0080 | 1.7500 | 0.9250 | 1.6200 | 1.7400 | 0.8933 | 0.2183 | Accepted | |
| $V_{avg}$ = 174.10 | 39540 | P [mm] | 12.0390 | 28.1090 | 6.7770 | 24.9000 | 27.9000 | 9.3159 | 58.1501 | Accepted | 0.0000 |
| $V_{max}$ = 175.13 | | O [deg] | 1.0170 | 1.8360 | 0.9410 | 1.6160 | 1.7970 | 0.9013 | 0.2213 | Accepted | |
| $V_{avg}$ = 149.42 | 46063 | P [mm] | 11.7830 | 27.7610 | 6.0340 | 24.3840 | 27.2290 | 8.7538 | 62.2023 | Accepted | 0.0000 |
| $V_{max}$ = 150.08 | | O [deg] | 1.0150 | 1.6490 | 0.9550 | 1.5350 | 1.6400 | 0.9062 | 0.2088 | Accepted | |
| $V_{avg}$ = 134.51 | 51273 | P [mm] | 10.4590 | 25.6890 | 5.3240 | 21.5690 | 25.2930 | 7.8093 | 48.3974 | Accepted | 0.0000 |
| $V_{max}$ = 135.05 | | O [deg] | 0.9980 | 1.6490 | 0.9250 | 1.5230 | 1.6370 | 0.8863 | 0.2104 | Accepted | |
| $V_{avg}$ = 124.65 | 55259 | P [mm] | 9.0610 | 22.0280 | 4.3860 | 19.2820 | 21.7880 | 6.6694 | 37.6254 | Accepted | 0.0000 |
| $V_{max}$ = 125.04 | | O [deg] | 0.9880 | 1.8010 | 0.9240 | 1.5560 | 1.7830 | 0.8752 | 0.2109 | Accepted | |
| $V_{avg}$ = 99.84 | 70447 | P [mm] | 7.9800 | 18.2900 | 4.2990 | 16.1770 | 18.1290 | 6.0265 | 27.3642 | Accepted | 0.0000 |
| $V_{max}$ = 100.07 | | O [deg] | 0.9320 | 1.8000 | 0.8770 | 1.4250 | 1.6420 | 0.8331 | 0.1749 | Accepted | |
| $V_{avg}$ = 49.97 | 143515 | P [mm] | 4.6940 | 11.1090 | 2.9370 | 9.0610 | 10.9780 | 3.6951 | 8.3816 | Accepted | 0.0000 |
| $V_{max}$ = 50.05 | | O [deg] | 0.9360 | 1.8080 | 0.8820 | 1.4140 | 1.6220 | 0.8343 | 0.1805 | Accepted | |
| $V_{avg}$ = 9.99 | 719274 | P [mm] | 3.5980 | 7.2880 | 2.4930 | 6.7290 | 7.2590 | 2.9391 | 4.3039 | Accepted | 0.0000 |
| $V_{max}$ = 10.05 | | O [deg] | 0.9640 | 1.8450 | 0.9070 | 1.5440 | 1.8090 | 0.8504 | 0.2052 | Accepted | |

P4 trajectory was unreliable and the respectively average velocity was 166.67 mm/s which is greater than the bound ($>$ 134.6 mm/s). For the controller, P3 was unreliable and the average velocity was 256.89 mm/s which is also greater

than the bound($>$ 247.61 mm/s). Thus, all the trajectories resulted in unreliable tracking data was found to have average velocities higher than the upper bounds thereby validating our obtained results on the dynamic performance bounds.

## V. CONCLUSION

This article provides an in-depth analysis of the spatial tracking performance of all the three HTC Vive VR tracking devices (tracker, controller, and HMD) through a series of standardized tests adapted from the ASTM's standard on the evaluation of the optical tracking system. The precision in static case was statistically inferred to have an average deviation $d_{avg}$ $<$1 $mm$, 0.5°, and maximum deviation $d_{max}$ $<$ 10 $mm$, 1°. The static case's accuracy was demonstrated statistically to have an average error $e_{avg}$ $<$3 $mm$, 0.5°, and maximum error $e_{max}$ $<$ 11 $mm$, 1°. The standard dynamic analysis procedure did not produce any significant statistical inference on the performance of the devices therefore a method derived from the standards was used to evaluate the reliable upper bound velocity. The reliability conditions were specified to consider both the quality (average error hypothesis test $H_0 < \delta_{avg}$) and the quantity (percentage loss $< 0.05\%$) of the tracking. In our case, we defined the $\delta_{avg}$ such that the devices are able to localize within itself, i.e., within their physical dimensions extremes. The upper bound results for each VLTS device were further substantiated with the random and complex human wrist motion trajectories recorded using Optitrack MOCAP and recreated in C16. As the choice of average error might be high for most of the applications, a procedure to validate the usage of VLTS for a custom application with a user-defined $\delta_{avg}$, and $\delta_{max}$ for both static and dynamic cases are described in the appendix along with few recommendations to configure VLTS.

## APPENDIX A
## PROCEDURE TO PERFORM STATIC PERFORMANCE EVALUATION FOR A CUSTOM APPLICATION

Here, we explain how to use our results to evaluate VLTS for a custom application for an expected average and maximum error. This is an adaption from the hypothesis test proposed in [22]. To perform static analysis, leftmargin=*

1) Select N $>$ 32 random pose within your workspace
2) Move your setup (robot or motion generator or just manually) with the device attached to these poses,
3) At each pose record the VLTS and the corresponding setup data (system to be tracked) (Note that if the data cannot be extracted from the system to be tracked, any other reference system can be used),
4) Calculate the error using the equation (1),
5) The above steps can be skipped if the error data for more than 32 pose exists,
6) Find $\bar{e}$ and $e_{max}$
7) Fix $\delta_{avg}$ and $\delta_{max}$ as per the average and maximum error the system is required to perform, (Note that if the interest is only on one of the values, the other value can be taken from the Table. 6)
8) Extract the $s^2$ for the specific device from the Table. 6,
9) Substitute the above values in the equation (2) and (3) to determine whether the null hypothesis of average error and maximum permissible error test is accepted or rejected,
10) If both the hypothesis is accepted, then we can concur that VLTS is suitable for the custom application and also the base stations are setup properly.
11) If any one of the hypothesis is rejected, then reconfigure the setup as per the recommendations mentioned later and repeat all the steps from the beginning until the hypothesis are accepted.

If the static analysis fails even after having the iterating with various configurations, then we can infer that VLTS is not the recommended system for the custom application to have an $\delta_{avg}$ and $e_{max}$. The next option is to increase the value of $\delta_{avg}$ and $e_{max}$, if the application can permit the increase in error and repeat the procedure.

## APPENDIX B
## PROCEDURE TO PERFORM DYNAMIC PERFORMANCE EVALUATION FOR A CUSTOM APPLICATION

Here, we describe the procedure to conduct dynamic performance analysis similar to section III-C3 for a custom application for an expected average error and percentage loss of data (Refer section III-C2). To perform dynamic analysis,

1) Select a trajectory based on the custom application with more than 32 samples (N$>$32 within your workspace) and an average velocity,
2) Perform the trajectory or motion with the tracking device attached,
3) At each pose record the VLTS and the corresponding setup data (system to be tracked),
4) Calculate the error using the equation (4) and (5).
5) Again, the above steps can be skipped if the error data exists for more than 32 samples,
6) Find $\bar{e}$,
7) Fix $\delta_{avg}$ and $\delta_{max}$ as per the average and maximum error the system is required to perform,
8) Calculate the percentage of loss in tracking (III-C1)
9) Extract the $s^2$ for the specific device from the Table. 14.
10) Substitute the above values in the equation (2),
11) Check whether the reliability condition is accepted or rejected (Refer section III-C2),
12) If the reliability conditions are accepted, then we can concur that VLTS is suitable for the custom application with error $\delta_{avg}$ and $\delta_{max}$,
13) If the reliability condition fails, check whether the average velocity of the trajectory is within the upper bound specified in section IV-C2. If the velocity is above the upper bound, we suggest to reduce the average velocity and repeat the procedure.

If the dynamic analysis fails repeatedly after reducing the velocity, then we can infer that the VLTS is not suitable for

the custom application to have $\delta_{avg}$ and $\delta_{max}$. The next option is to increase the value of $\delta_{avg}$ and $e_{max}$, if the application can allow increase in error and repeat the procedure.

## APPENDIX C
## RECOMMENDATIONS FOR VLTS SETUP

Along with the considerations mentioned in section II-A which includes the vendor's suggestions, we recommend the following to be taken into account while configuration

- Ensure that the sweep of the base station reaches the entire volume of work by specifying the workspace to track into a cube (play area * height). The best way to get this area completely enclosed is to have the base stations at the end of the play area diagonal. The most common error is to place the base stations at the midpoints of the cube's edges, this configuration would significantly decrease the tracking efficiency at the play area edges.
- Ensure the tracking devices are consistently visible to at least one of the base stations. It is better to make the devices visible to only one base station than visibility limited for both.
- Assign a unique role to the trackers and controller. This will ensure that the data received is not corrupted. For instance, if the role of ''left-hand'' is assigned to a tracker and a controller then the data from both these devices may be interchanged leading to swapping in visual and pose data of ''left-hand'' interpreted. This depends on the software application written to receive the data but we still suggest that the roles should be kept different from one another.
- The order from which each device is connected defines the SteamVR identification number. So if a series of experiments are carried out, the best way to maintain the Id's order is to connect the same way it was first paired. This is highly recommended for using VLTS as a MOCAP solution.

These recommendations are made from observations and rectifying the failures while conducting this extensive study.

## ACKNOWLEDGMENT

The authors would like to acknowledge the contributions of Michal Jilich and Keerthi Sagar of PMAR Robotics Group members for their assistance in tool mount design and non-synthetic trajectory data collection.

## REFERENCES

[1] *R/Vive—Vive Lighthouse Explained*. Accessed: May 2019. [Online]. Available: https://www.reddit.com/r/Vive/comments/40877n/vive_lighthouse_explained/
[2] S. M. LaValle, A. Yershova, M. Katsev, and M. Antonov, ''Head tracking for the oculus rift,'' in *Proc. IEEE Int. Conf. Robot. Autom. (ICRA)*, May 2014, pp. 187–194.
[3] J. Hesch, ''Powered by Ai: Oculus insight,'' Facebook AI, Menlo Park, CA, USA, Tech. Rep., Aug. 2019. [Online]. Available: https://ai.facebook.com/blog/powered-by-ai-oculus-insight/
[4] J. P. Rolland *et al.*, ''A survey of tracking technology for virtual environments,'' *Fundam. Wearable Comput. Augmented Reality*, vol. 1, no. 1, pp. 67–112, 2001.
[5] K. Dorfmüller and H. Wirth, ''Real-time hand and head tracking for virtual environments using infrared beacons,'' in *Proc. Int. Workshop Capture Techn. Virtual Environ.* Berlin, Germany: Springer, 1998, pp. 113–127.
[6] K. Dorfmüller, ''Robust tracking for augmented reality using retroreflective markers,'' *Comput. Graph.*, vol. 23, no. 6, pp. 795–800, Dec. 1999.
[7] (May 2017). *Inside-Out V Outside-in: How VR Tracking Works, and How it's Going to Change*. [Online]. Available: https://www.wareable.com/vr/inside-out-vs-outside-in-vr-tracking-343
[8] M. Borges, A. Symington, B. Coltin, T. Smith, and R. Ventura, ''HTC Vive: Analysis and accuracy improvement,'' in *Proc. IEEE/RSJ Int. Conf. Intell. Robots Syst. (IROS)*, Oct. 2018, pp. 2610–2615.
[9] T. A. Jost, G. Drewelow, S. Koziol, and J. Rylander, ''A quantitative method for evaluation of 6 degree of freedom virtual reality systems,'' *J. Biomechanics*, vol. 97, Dec. 2019, Art. no. 109379.
[10] D. C. Niehorster, L. Li, and M. Lappe, ''The accuracy and precision of position and orientation tracking in the HTC Vive virtual reality system for scientific research,'' *i-Perception*, vol. 8, no. 3, pp. 1–23, 2017.
[11] E. Luckett, ''A quantitative evaluation of the HTC Vive for virtual reality research,'' Ph.D. dissertation, Dept. Comput. Inf. Sci., Univ. Mississippi, Oxford, MS, USA, 2018.
[12] S. van der Veen, M. Bordeleau, P. Pidcoe, C. France, and J. Thomas, ''Agreement analysis between Vive and vicon systems to monitor lumbar postural changes,'' *Sensors*, vol. 19, no. 17, p. 3632, Aug. 2019.
[13] T. Ameler, M. Warzecha, D. Hes, J. Fromke, A. Schmitz-Stolbrink, C. M. Friedrich, K. Blohme, L. Brandt, R. Brungel, A. Hensel, L. Huber, F. Kuper, J. Swoboda, and M. Warnecke, ''A comparative evaluation of SteamVR tracking and the OptiTrack system for medical device tracking,'' in *Proc. 41st Annu. Int. Conf. IEEE Eng. Med. Biol. Soc. (EMBC)*, Jul. 2019, pp. 1465–1470.
[14] K. Sletten, ''Automated testing of industrial robots using HTC Vive for motion tracking,'' M.S. thesis, Dept. Elect. Comput. Eng., Univ. Stavanger, Stavanger, Norway, 2017.
[15] HTC. (Jun. 2020). *Vive Tracker Developer Guidelines*. [Online]. Available: https://developer.vive.com/resources/knowledgebase/vive-tracker-developer-guidelines/
[16] M. Le Chénéchal and J. Chatel-Goldman, ''HTC Vive Pro time performance benchmark for scientific research,'' ICAT-EGVE, Limassol, Cyprus, Tech. Rep. ffhal-01934741, Nov. 2018.
[17] M. Greiff, A. Robertsson, and K. Berntorp, ''Performance bounds in positioning with the VIVE lighthouse system,'' in *Proc. 22th Int. Conf. Inf. Fusion (FUSION)*, Jul. 2019, pp. 1–8.
[18] Y. Yang, D. Weng, D. Li, and H. Xun, ''An improved method of pose estimation for lighthouse base station extension,'' *Sensors*, vol. 17, no. 10, p. 2411, Oct. 2017.
[19] M. Suznjevic, M. Mandurov, and M. Matijasevic, ''Performance and QoE assessment of HTC vive and oculus rift for pick-and-place tasks in VR,'' in *Proc. 9th Int. Conf. Qual. Multimedia Exper. (QoMEX)*, May 2017, pp. 1–3.
[20] *ASTM Standard*. Accessed: Feb. 2020. [Online]. Available: https://www.astm.org/
[21] *Standard Practice for Use of the Terms Precision and Bias in ASTM Test Methods*, Standard E177-19, West Conshohocken, PA, doi: 10.1520/E0177-19.
[22] *Standard Test Method for Evaluating the Performance of Systems That Measure Static, Six Degrees of Freedom (6DOF), Pose*, Standard ASTM-E2919-14, ASTM International, West Conshohocken, PA, 2014. [Online]. Available: http://www.astm.org/cgi-bin/resolver.cgi?E2919
[23] *Standard Test Method for Evaluating the Performance of Optical Tracking Systems That Measure Six Degrees of Freedom (6DOF) Pose*, Standard ASTM-E3064-16, ASTM International, West Conshohocken, PA, 2016. [Online]. Available: http://www.astm.org/cgi-bin/resolver.cgi?E3064
[24] (Dec. 2016). *Alan Yates on the Impossible Task of Making Valve's VR Work*. [Online]. Available: https://www.youtube.com/watch?v=75ZytcYANTA
[25] (Dec. 2015). *Ns-16-1.65: Characteristics and Technical Specifics*. [Online]. Available: https://www.comau.com/IT/le-nostre-competenze/robotics/robot-team/ns-16-165
[26] P. Merriaux, Y. Dupuis, R. Boutteau, P. Vasseur, and X. Savatier, ''A study of vicon system positioning performance,'' *Sensors*, vol. 17, no. 7, p. 1591, Jul. 2017.
[27] B. Sabata and J. K. Aggarwal, ''Estimation of motion from a pair of range images: A review,'' *CVGIP: Image Understand.*, vol. 54, no. 3, pp. 309–324, Nov. 1991.

[28] D. W. Eggert, A. Lorusso, and R. B. Fisher, "Estimating 3-D rigid body transformations: A comparison of four major algorithms," *Mach. Vis. Appl.*, vol. 9, nos. 5–6, pp. 272–290, Mar. 1997.
[29] S. Umeyama, "Least-squares estimation of transformation parameters between two point patterns," *IEEE Trans. Pattern Anal. Mach. Intell.*, vol. 13, no. 4, pp. 376–380, Apr. 1991.
[30] J. Cashbaugh and C. Kitts, "Automatic calculation of a transformation matrix between two frames," *IEEE Access*, vol. 6, pp. 9614–9622, 2018.
[31] *Valvesoftware/Openvr Github Repository*. Accessed: Jan. 2020. [Online]. Available: https://github.com/ValveSoftware/openvr
[32] *Vlts Evaluation System Github Repository*. Accessed: Sep. 14. [Online]. Available: https://github.com/MSIhub/Vive_SpatialTrackingStudy.git
[33] W. M. Mendenhall and T. L. Sincich, *Statistics for Engineering and the Sciences*. Boca Raton, FL, USA: CRC Press, 2016.
[34] M. L. Head, L. Holman, R. Lanfear, A. T. Kahn, and M. D. Jennions, "The extent and consequences of P-Hacking in science," *PLOS Biol.*, vol. 13, no. 3, Mar. 2015, Art. no. e1002106.
[35] (Jan. 2015). *International Organization for Standardization*. [Online]. Available: https://www.iso.org/standard/22244.html

**MOHAMED SADIQ IKBAL** received the B.Tech. degree in mechanical engineering from Pondicherry University, Puducherry, India, in 2014, and the dual Erasmus Mundus master's degree in advanced robotics from the Ecole Centrale de Nantes, France, and the University of Genoa, Italy, in 2017. He is currently pursuing the Ph.D. degree in mechanics, robotics, and measurements curriculum with the University of Genoa, Italy.

He worked as a Systems Engineer Trainee with Tata Consultancy Service, Chennai, India, in 2015. His research interests include development of robotic motion platform for virtual reality-based motion simulator, motion perception algorithms, human interaction in virtual reality, design of experimentation, and development of mechanism simulation software. He received the Gold Medal for his B.Tech. degree from Pondicherry University, in 2014.

**VISHAL RAMADOSS** (Member, IEEE) was born in Chennai, Tamil Nadu, India, in 1990. He received the B.E. degree in electrical and electronics engineering from Anna University, Chennai, in 2011, the master's degree in control and robotics from the Ecole Centrale de Nantes, France, in 2014, the master's degree in robotics engineering and the Ph.D. degree in mechanical engineering and robotics from the University of Genoa, Italy, in 2015 and 2020, respectively.

He is currently a Postdoctoral Fellow with the PMAR Robotics Group, Department of Mechanical, Energy, Management, and Transportation Engineering, University of Genoa. His research interests include kinematics and design of redundantly actuated complex mechanisms, musculoskeletal robots, rehabilitation and biomechatronics, tensegrity robots, and human–robot interaction.

**MATTEO ZOPPI** received the degree in mechanical engineering from the University of Genoa, in 2000, and the Ph.D. degree in robotics in 2003.

Since the end of 2014, he has been a Second Level University Professor with the Department of Mechanical Engineering, University of Genoa, where he is currently an Associate Professor with the DIME–PMAR Robotics Group. His teachings include functional mechanical design, modeling of mechanical systems, mechanical design methods in robotics, and advanced modeling and simulation of mechanical systems. His scientific activities are also aimed at the methods of synthesis and analysis of mechanisms for robotics, screw theory in robotics, and design and development of robotic and automation systems.